Supporting information

for the article:

3D printing for safe organic synthesis in mixed liquid/gas-phase chemistry

Victoria A. Korabelnikova,[a] Yulia V. Gyrdymova,[b] Evgeniy G. Gordeev,[a] Anton N. Potorochenko,[b] Konstantin S. Rodygin[b] and Valentine P. Ananikov[a]*

[a]Zelinsky Institute of Organic Chemistry, Russian Academy of Sciences, Leninsky Pr. 47, Moscow 119991, Russia; http://AnanikovLab.ru

[b]Saint Petersburg State University, 7/9 Universitetskaya nab., St. Petersburg, 199034 Russia

*val@ioc.ac.ru

Content

1. Design of 3D-printable chemical reactors for liquid/gas-phase organic synthesis

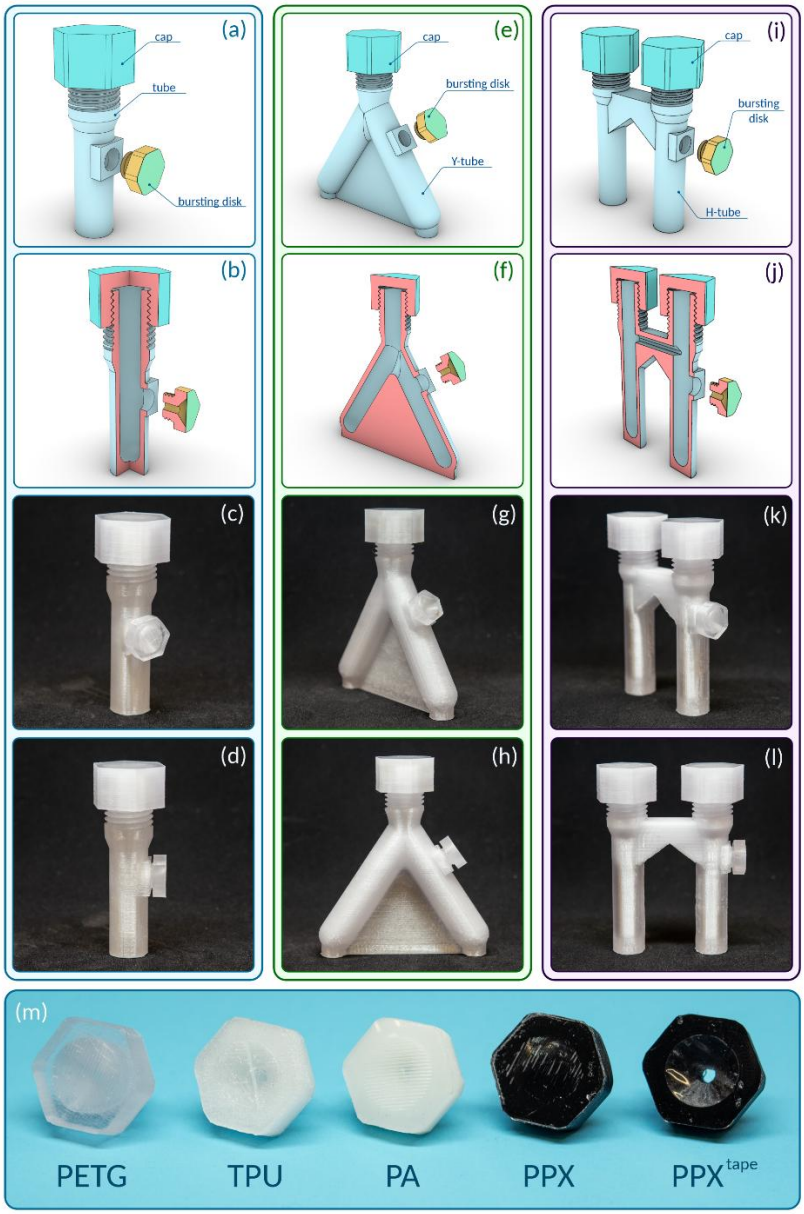

Figure S1. The safety module with a bursting disc integrated into the reactor base: (a) 3D model of the I-tube reactor with a cap and safety module with a bursting disc; (b) sectional view of the I-tube reactor with a cap and safety module with a bursting disc; (c), (d) ready-to-use I-tube reactor with a cap and safety module with a bursting disc made of PETG, with a reactor wall thickness of 3 mm; (e) 3D model of the Y-tube reactor with a cap and safety module with a bursting disc; (f) sectional view of the Y-tube reactor with a cap and safety module with a bursting disc; (g), (h) ready-to-use Y-tube reactor with a cap and safety module with a bursting disc made of PETG, with a reactor wall thickness of 3 mm; (i) 3D model of the H-tube reactor with a cap and safety module with a bursting disc; (g) sectional view of the H-tube reactor with a cap and safety module with a bursting disc; (k), (l) ready-to-use H-tube reactor with a cap and safety module with bursting disc made of PETG, reactor wall thickness 3 mm; (m) safety module with a bursting disc made of PETG, TPU, PA, PPX (in the PPX^{tape} module, the bursting disc is a transparent polypropylene scotch tape).

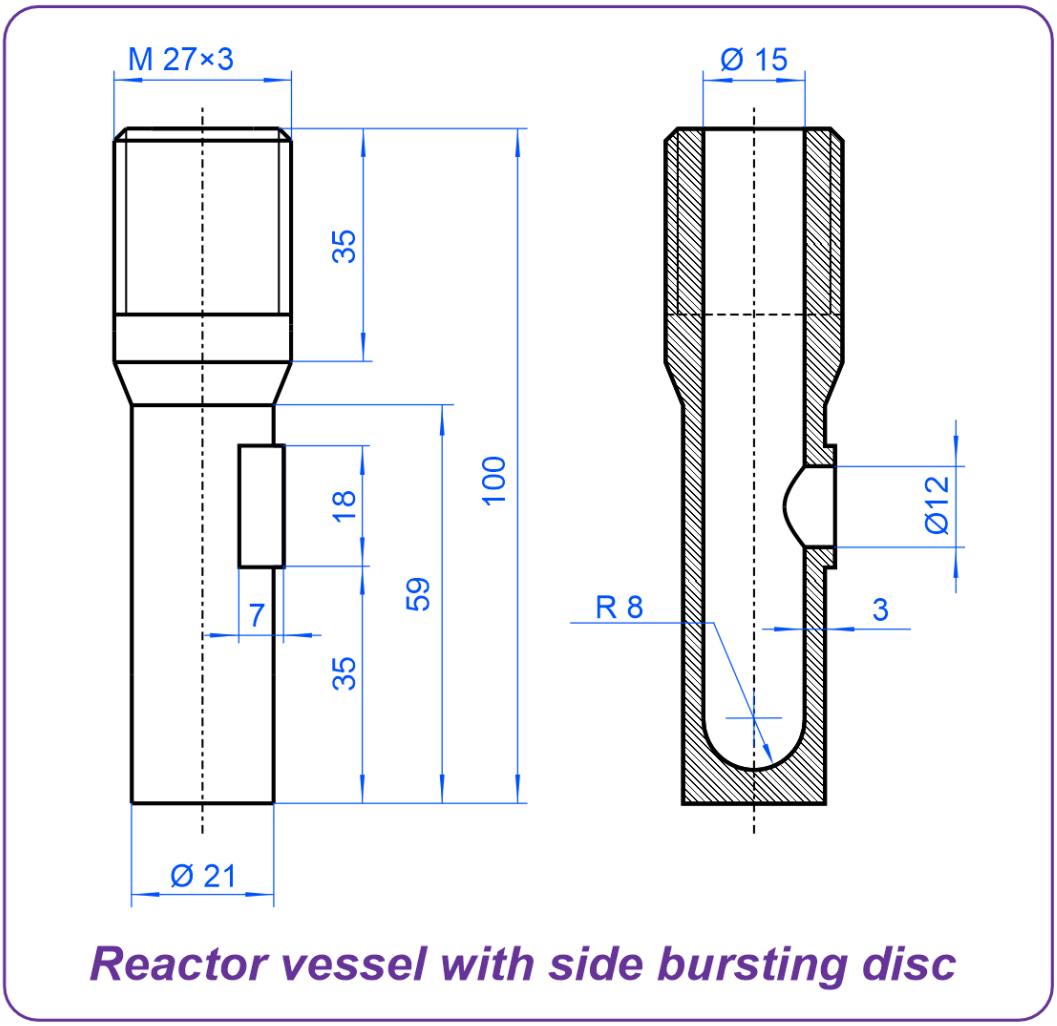

Figure S2. Drawing of the I-tube type 1 reactor vessel with a side bursting disc.

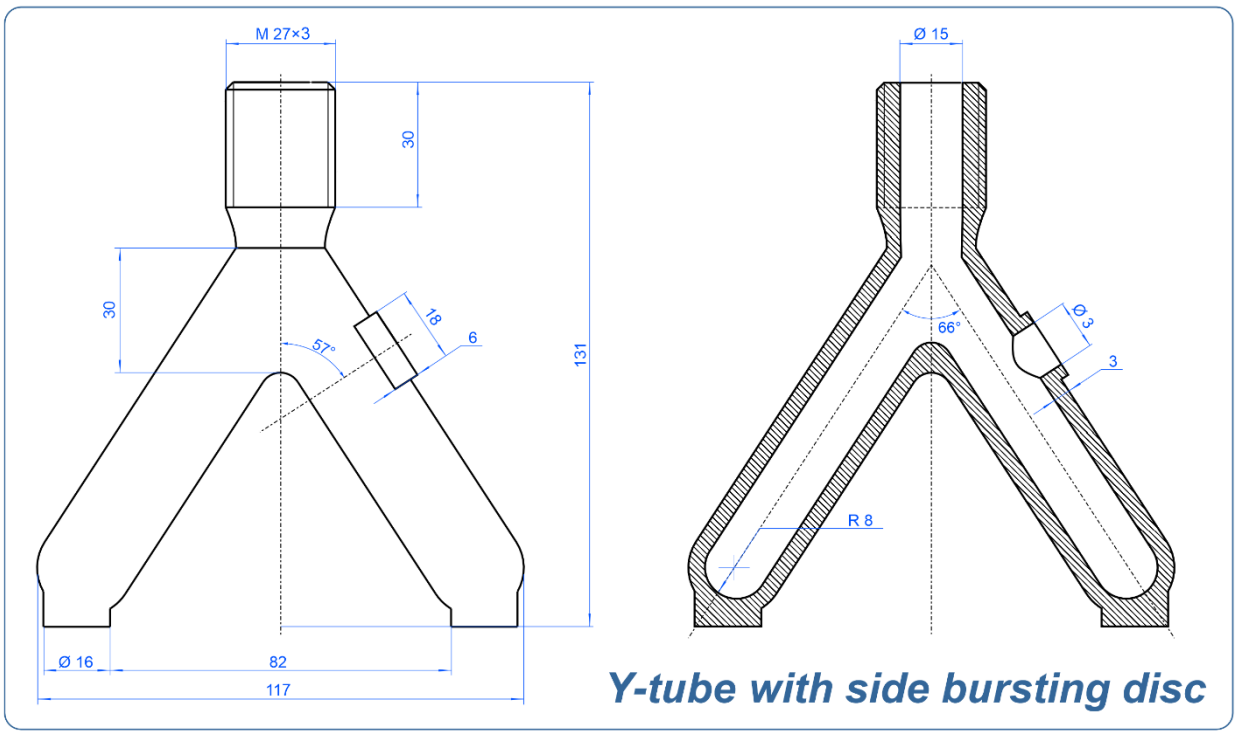

Figure S3. Drawing of the Y-tube type 1 reactor vessel with a side bursting disc.

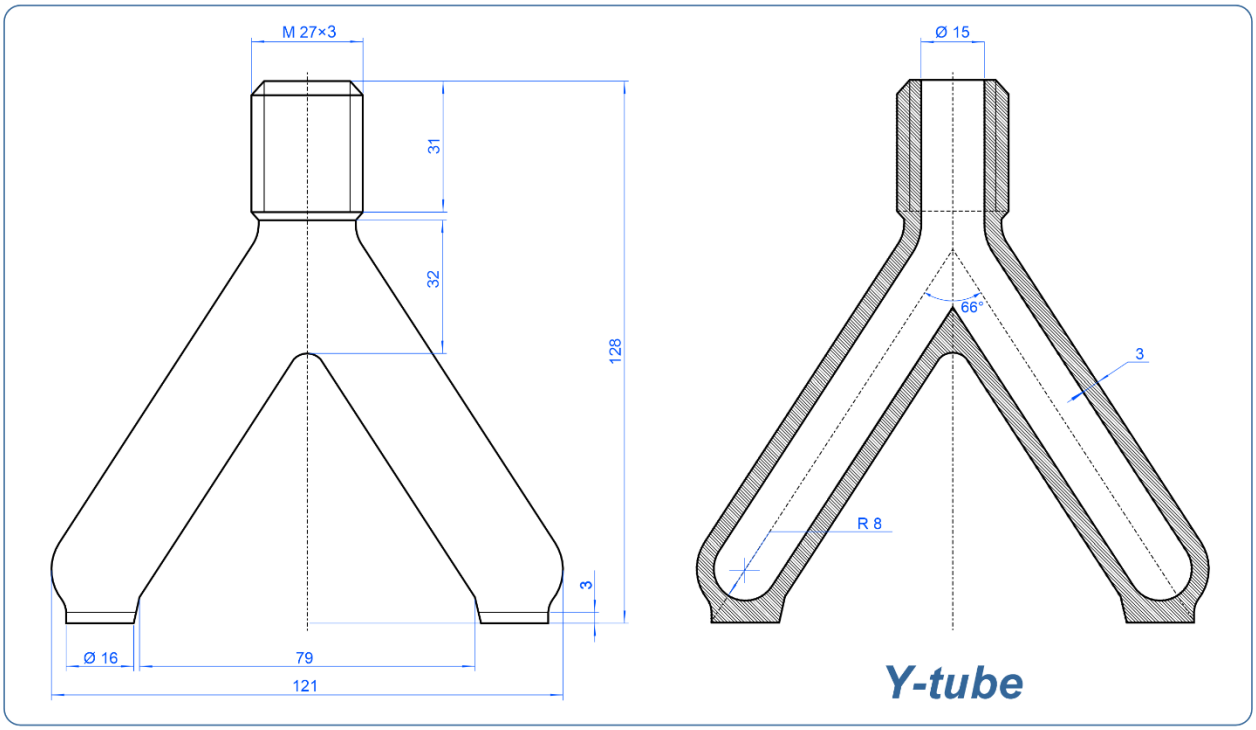

Figure S4. Drawing of the Y-tube type 2 reactor vessel.

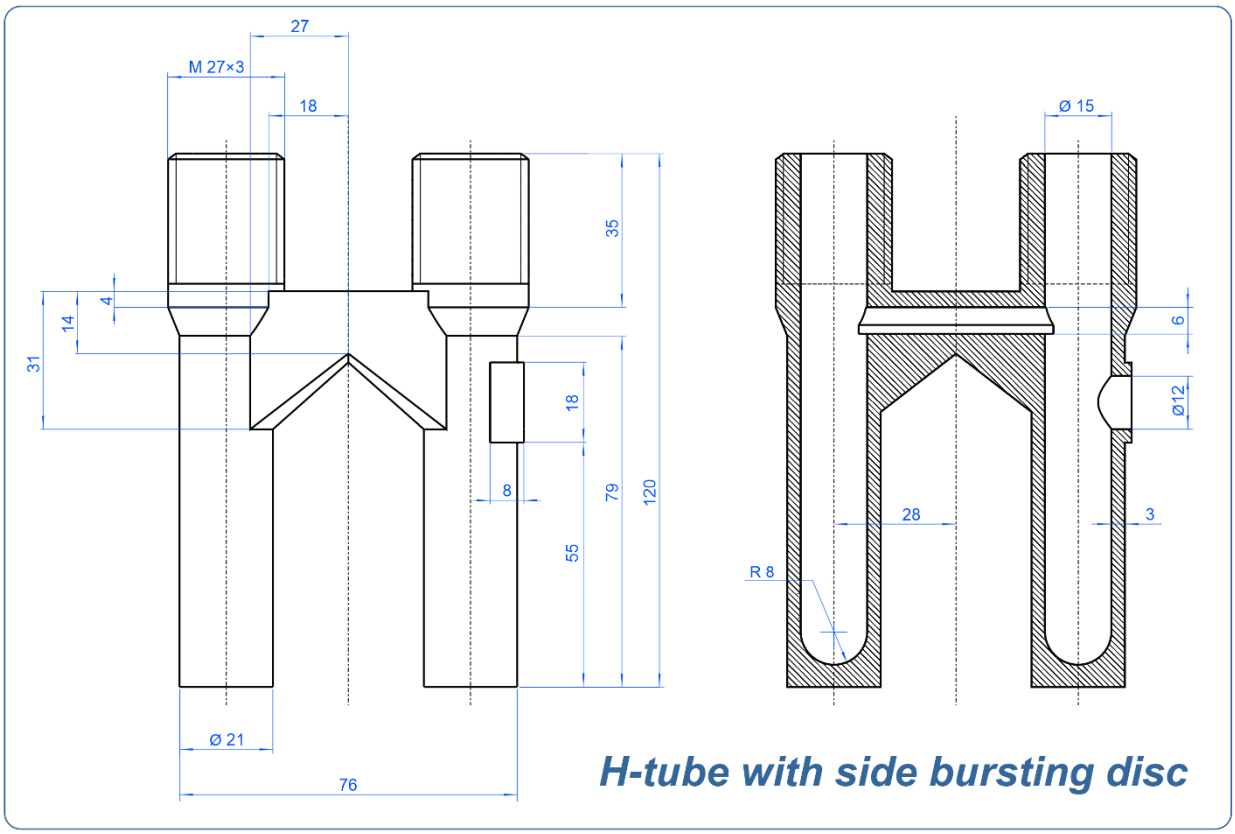

Figure S5. Drawing of reactor vessel H-tube type 1 with a side bursting disc.

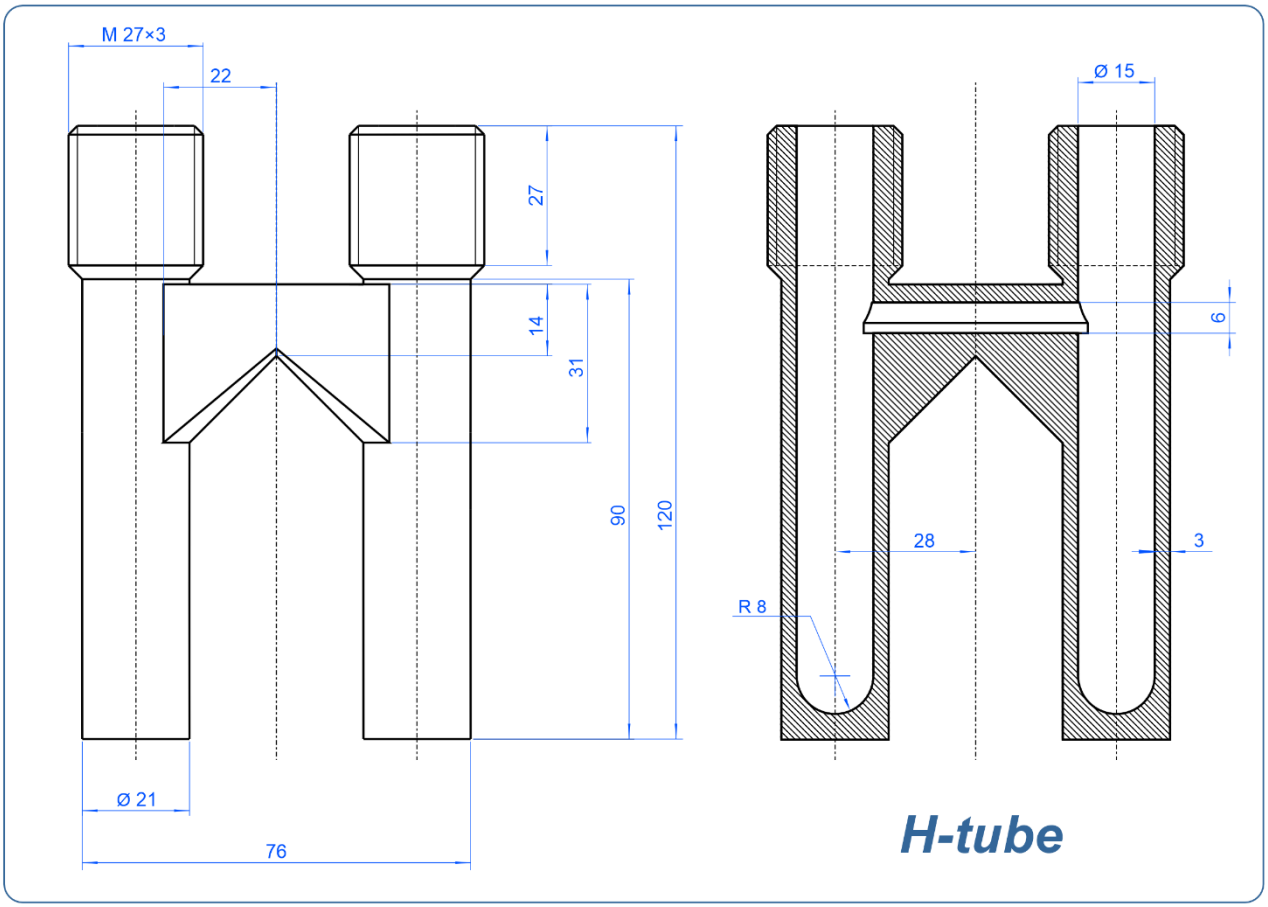

Figure S6. Drawing of reactor vessel H-tube type 2.

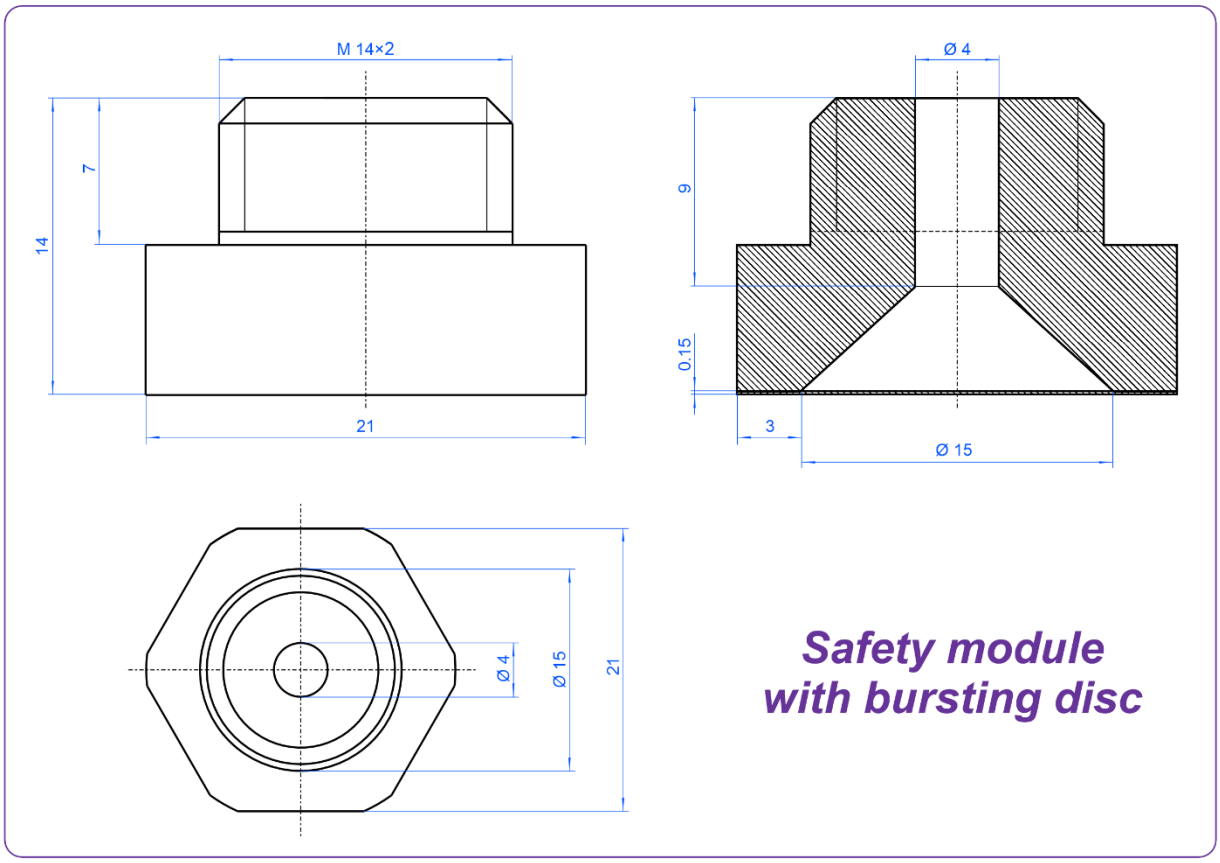

Figure S7. Drawing of the safety module with a bursting disc.

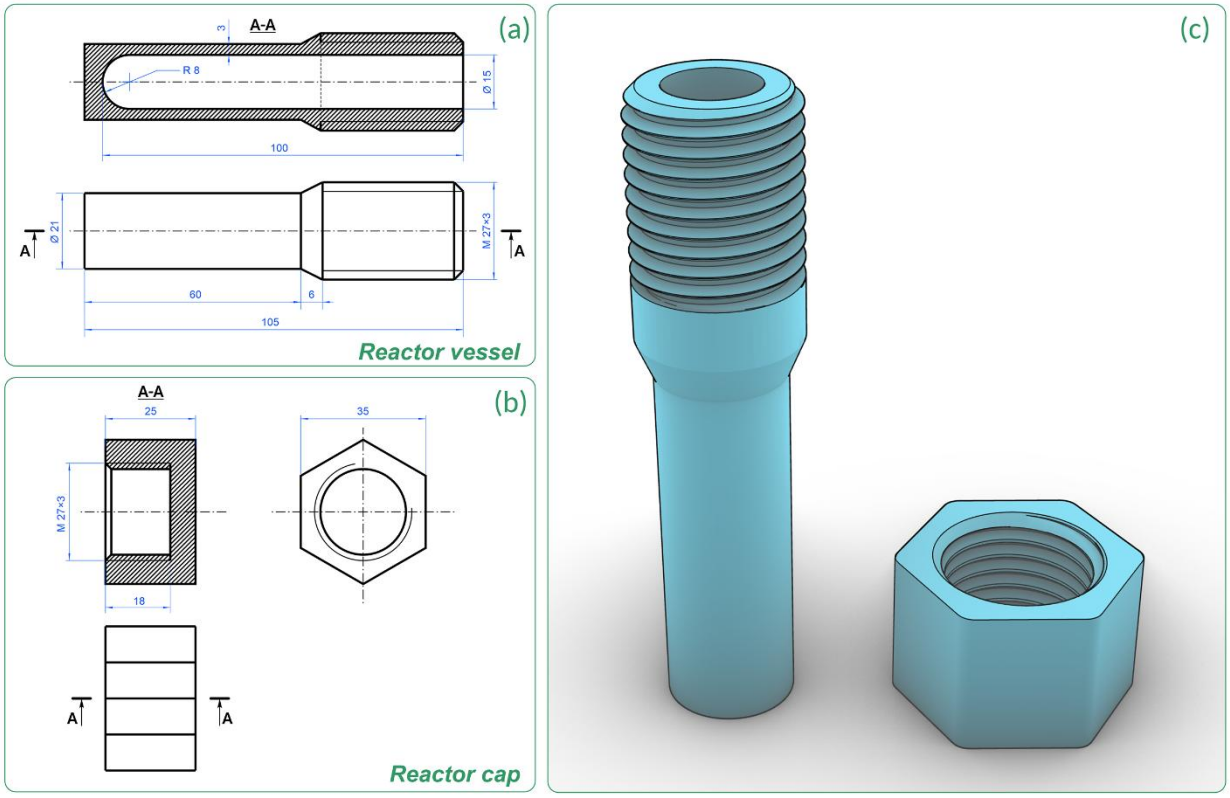

Figure S8. (a) Drawing of the I-tube type 2 reactor vessel; (b) reactor cap drawing; (c) general view of the I-tube type 3 reactor model.

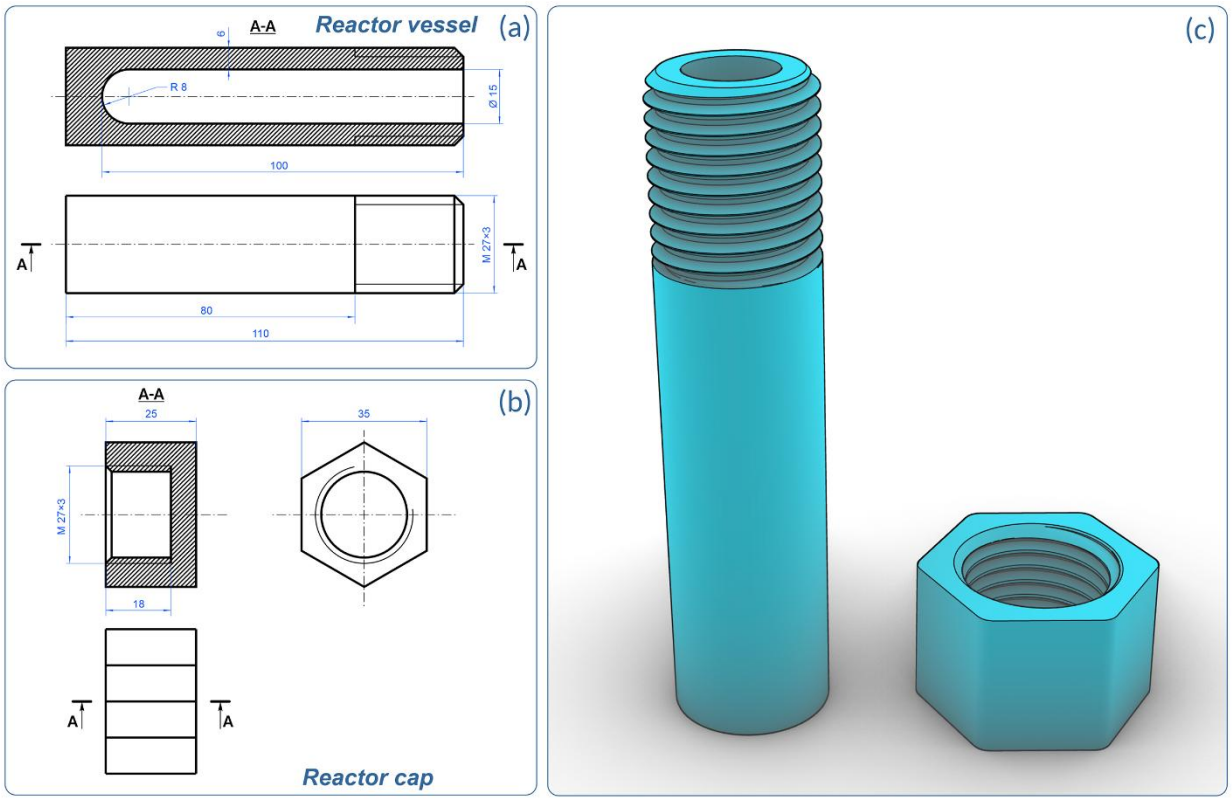

Figure S9. (a) Drawing of the I-tube type 3 reactor vessel; (b) reactor cap drawing; (c) general view of the I-tube type 2 reactor model.

Figure S10. Reactors with standard thread M27 (type 2). The figure shows the finished design of parts made of PETG, PP-GF30, PA-CF and stainless nonmagnetic steel AISI 321 with high corrosion resistance.

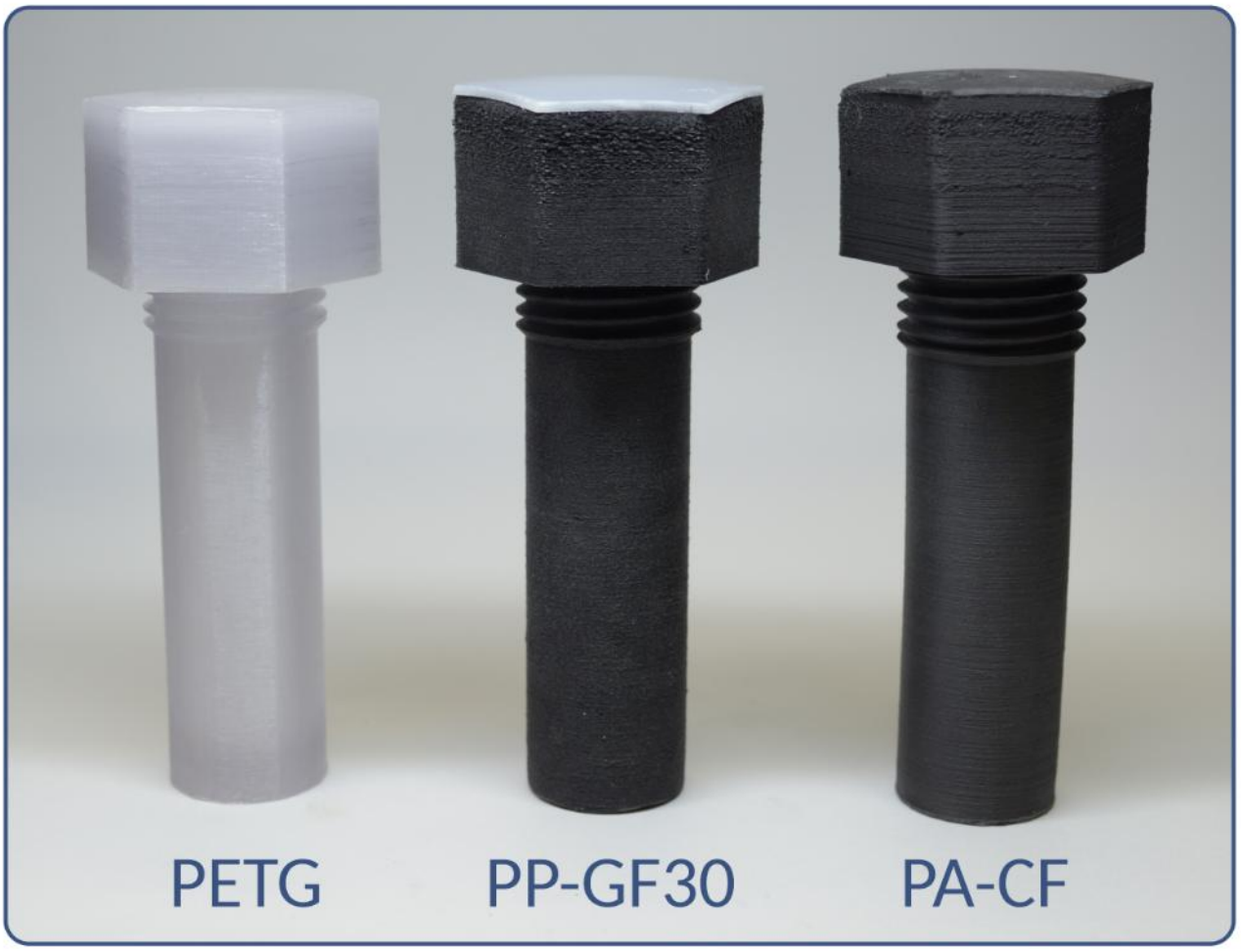

Figure S11. Large-volume reactors (100 ml). The figure shows the final design of the PETG, PP-GF30, and PA-CF products.

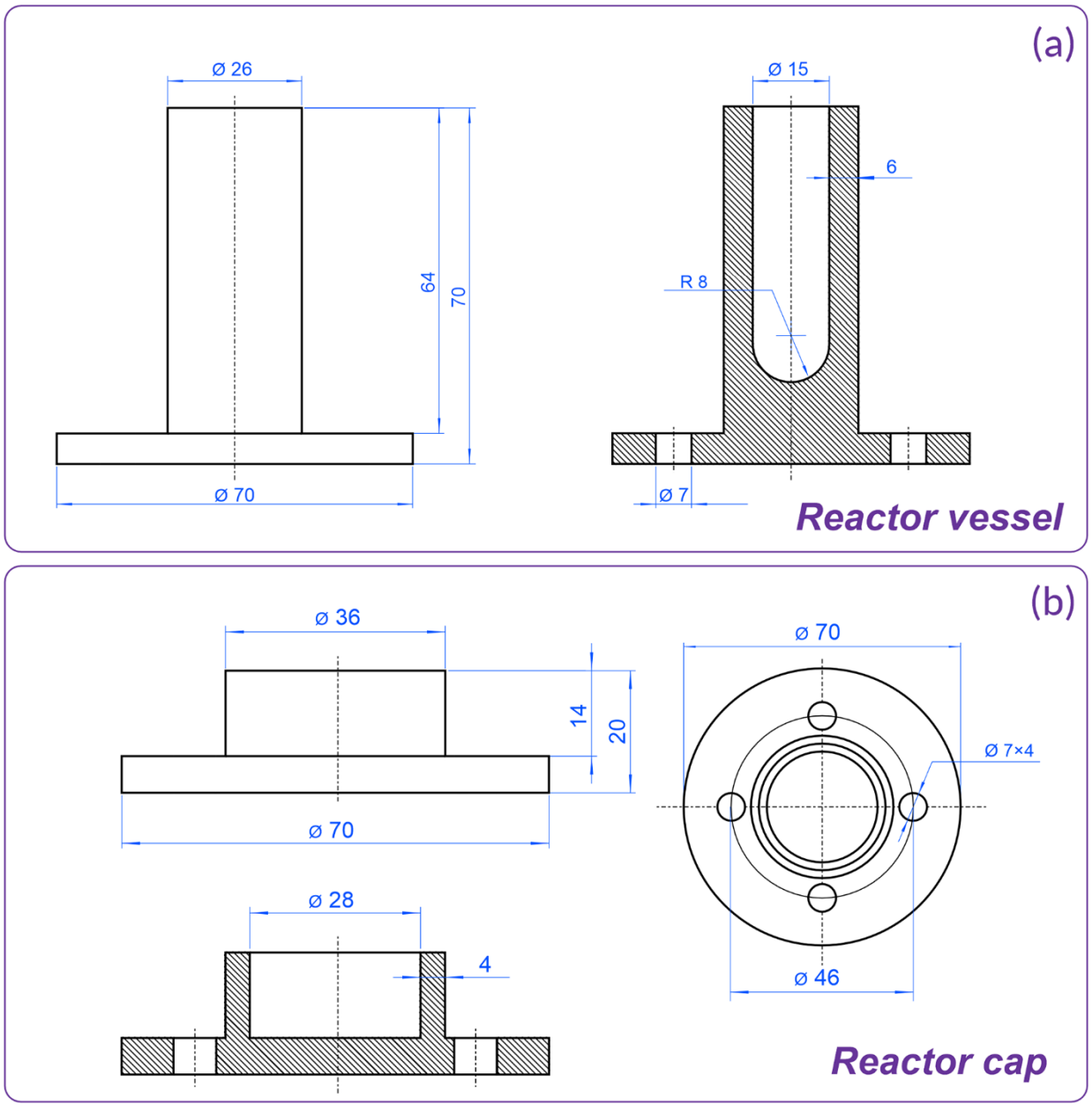

Figure S12. (a) Drawing of the I-tube type 4 reactor vessel; (b) drawing of the reactor cap.

2. Physical tests of the FFF reactors

2.1 Impermeability tests

Figure S13. Impermeability tests inside alcohol media for I-tube type 3 (a-c) and I-tube type 4 reactors made of PETG (d, e).

Figure S14. Impermeability tests inside alcohol media for I-tube type 3 (a-c) and I-tube type 4 reactors made of PP-GF30 (d, e).

2.2 Strength tests of the bursting discs

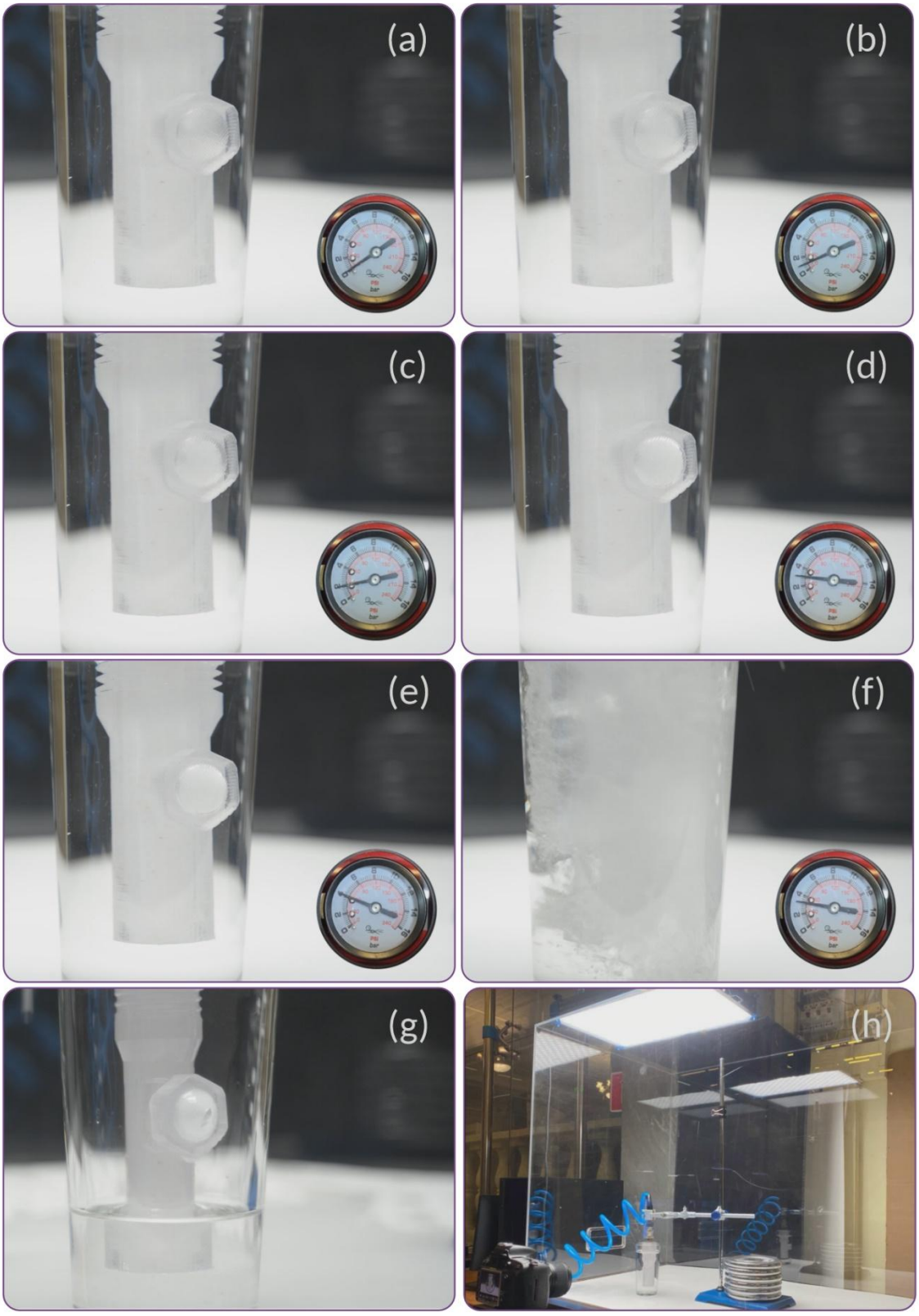

Figure S15. Testing of a safety module with a bursting disc under an overpressure of air: (a) test start (0 bar); (b-e) pressure increase up to 4 bar; (f) bursting point; (g) bursting disc after destruction; (h) testing stand.

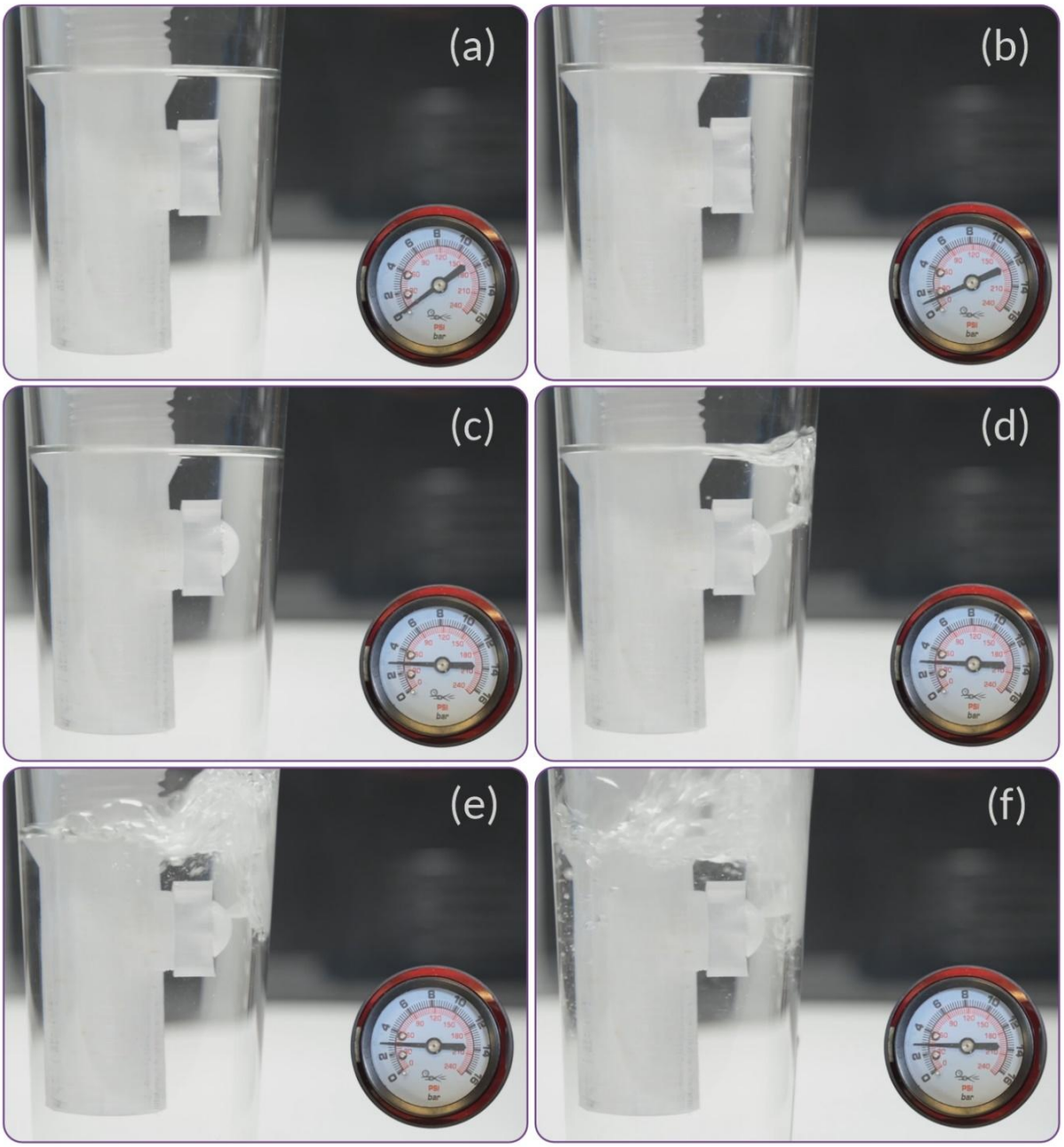

Figure S16. Testing of a safety module with a bursting disc under overpressure of air: (a) test start (0 bar); (b, c) pressure increase and bursting disc deformation; (d) bursting point; (e, f) gradual decrease in the pressure inside the reactor due to disc destruction.

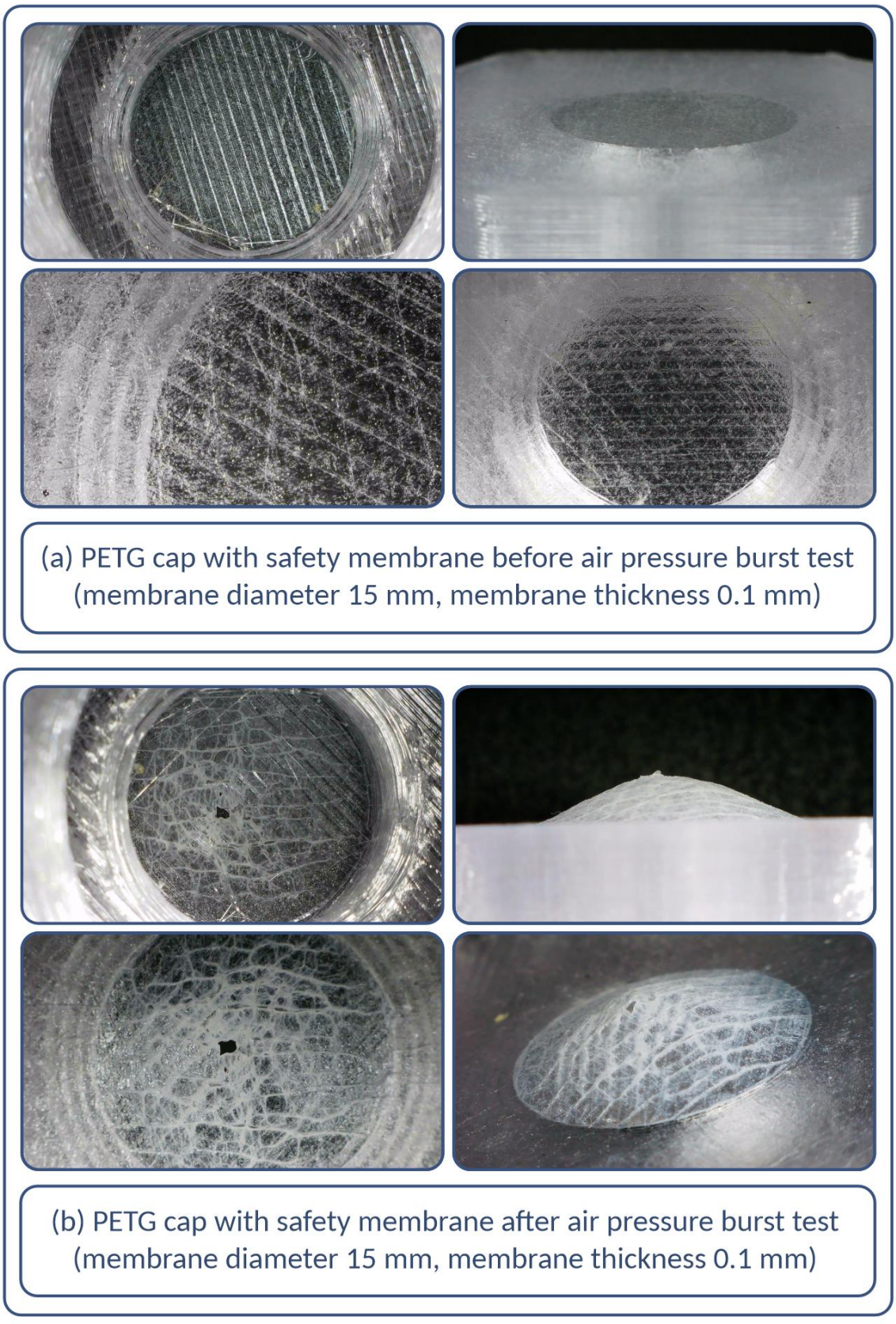

Figure S17. PETG cap with a bursting disc (a) before and (b) after the burst test under overpressure of air (disc diameter 15 mm, thickness 0.1 mm).

Table S1. Optimization of pressure relief bursting discs parameters.

	Disc diameter, mm	Disc thickness, mm	Extrusion width (w), mm	Extrusion multiplier (k-value)	Impermeability (bar)	Disc rupture at (bar)
PETG						
1	5	0.25	0.63	0.98	7.5)	>7.5
2	10	0.15	0.63	0.98	7.5	>7.5
3	12	0.05	0.63	0.98	no	–
4	12	0.05	0.67	1.00	no	–
5	12	0.1	0.67	1.00	7.5	>7.5
6	15	0.07	0.67	1.00	no	–
7	15	0.05	0.67	1.02	< 1.0	≈ 1.0
8	15	0.07	0.67	1.02	1.5	2.0
9	15	0.1	0.67	1.02	4.0	5.0
PP-GF30						
1	15	0.05	0.7	1.05	1.0	2.0
2	15	0.07	0.7	1.05	5.0	6-7
3	15	0.1	0.7	1.05	7.5	>7.5
PA-CF						
1	15	0.05	0.7	1.02	1.0	≈ 1.5
2	15	0.07	0.7	1.02	2.0	3.0
3	15	0.1	0.7	1.02	7.5	>7.5

Table S2. Burst pressure values (bar) for 20 bursting discs of 15 mm in diameter and 0.1 mm in thickness made of PETG. *

1	2	3	4	5	6	7	8	9	10
4.8	5.4	4.8	4.6	4.8	4.8	5.2	5.1	4.9	5.2
11	12	13	14	15	16	17	18	19	20
5.1	5.2	5.3	5.2	5.5	4.7	4.7	5.3	4.8	4.8

*Printing parameters: extrusion width - 0.8 mm; extrusion multiplier - 1.02; and bed temperature for the first layer - 265 °C.

Table S3. Results of bursting disc breakage experiments with acetylene formed by *in situ* hydrolysis of calcium carbide.

n (CaC_2), mmol	V (H_2O), µL	PP-GF30			PA-CF		PETG	
		0.05	0.07	0.1	0.07	0.1	0.07	0.1
1	37	●	●	●	●	●	●	●
2	74	●	●	●	●	●	●	●
3	110	●	●	●	●	●	●	●
4	147	●	●	●	●	●	●	●
5*	185*	●	●	●	●	●	●	●
6	222	●	●	●	●	●	●	●
7	259	●	●	●	●	●	●	●
8*	296*	●	●	●	●	●	●	●
9	333	●	●	●	●	●	●	●
10	370	●	●	●	●	●	●	●
11*	407*	●	●	●	●	●	●	●
12	444	●	●	●	●	●	●	●
13	481	●	●	●	●	●	●	●

*Parameters of the experiment at which disc rupture occurred: ● – disc is impermeable; ● – disc rupture.

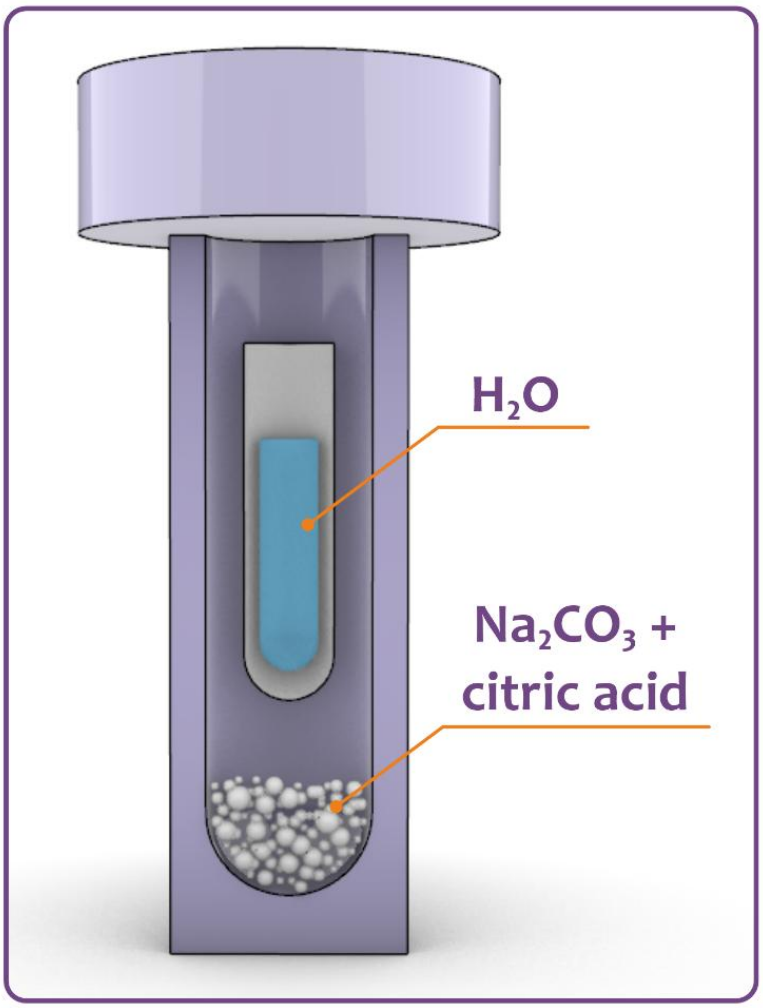

Figure S18. Schematic illustration of a reactor for the reaction of sodium carbonate with citric acid to form CO_2.

$$3\ Na_2CO_3 + 2\ (HOOCCH_2)C(OH)COOH \longrightarrow 3\ CO_2 + 3\ H_2O + (NaOOCCH_2)C(OH)COONa$$

Scheme S1. Sodium carbonate reacts with citric acid to form carbon dioxide.

Table S4. Experimental results on disc strength using CO_2.

n (Na_2CO_3), mmol	m (Na_2CO_3), mg	m (citric acid), mg	PP-GF30			PA-CF		PETG	
			0.05	0.07	0.1	0.07	0.1	0.07	0.1
1	106	130	●	●	●	●	●	●	●
2	212	260	●	●	●	●	●	●	●
3*	318*	320*	●	●	●	●	●	●	●
4	424	520	●	●	●	●	●	●	●
5*	530*	650*	●	●	●	●	●	●	●
6*	636*	780*	●	●	●	●	●	●	●
7*	742*	910*	●	●	●	●	●	●	●
8*	848*	1040*	●	●	●	●	●	●	●
9*	954*	1170*	●	●	●	●	●	●	●

*Parameters of the experiment at which disc breakage occurred: ● - disc is impermeable; ● - disc fracture.

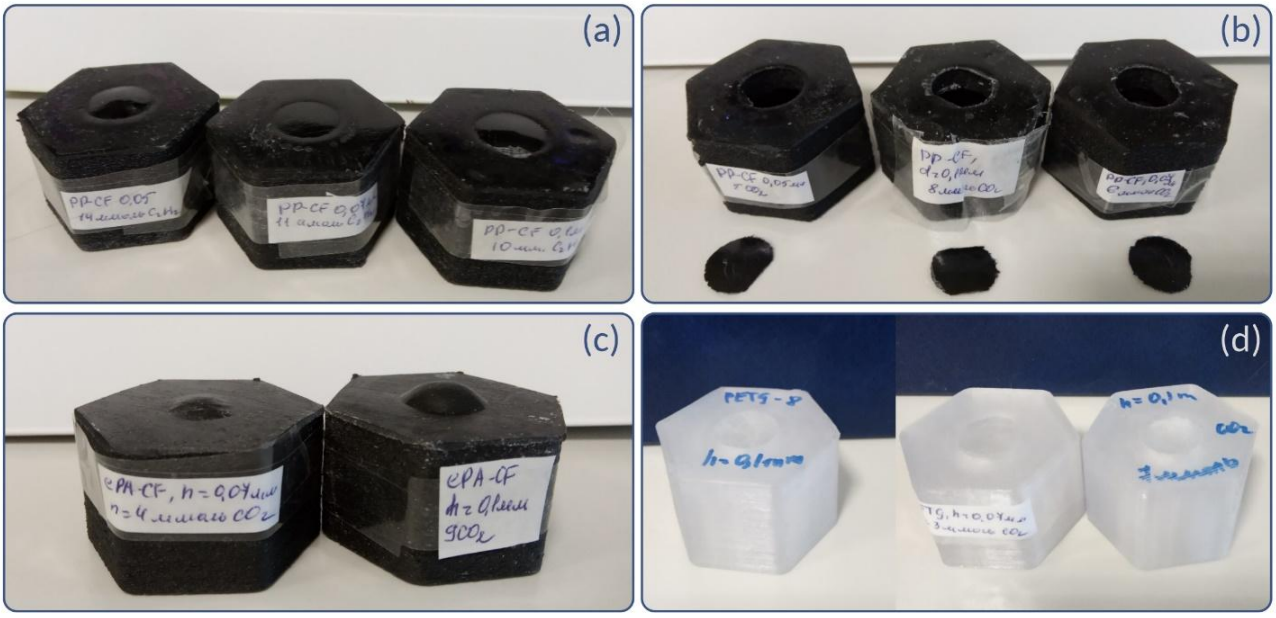

Figure S19. (a) PP-GF30 caps with different disc thicknesses (0.05, 0.07, and 0.1 mm) after the end of the CaC_2 experiment; (b) PP-GF30 caps with different disc thicknesses (0.05, 0.07, and 0.1 mm) after the end of the CO_2 experiment; (c) PA-CF caps with different disc thicknesses (0.07 and 0.1 mm) after the end of the CO_2 experiment; (d) PETG caps with different disc thicknesses (0.07 and 0.1 mm) after the end of the CaC_2 and CO_2 experiments.

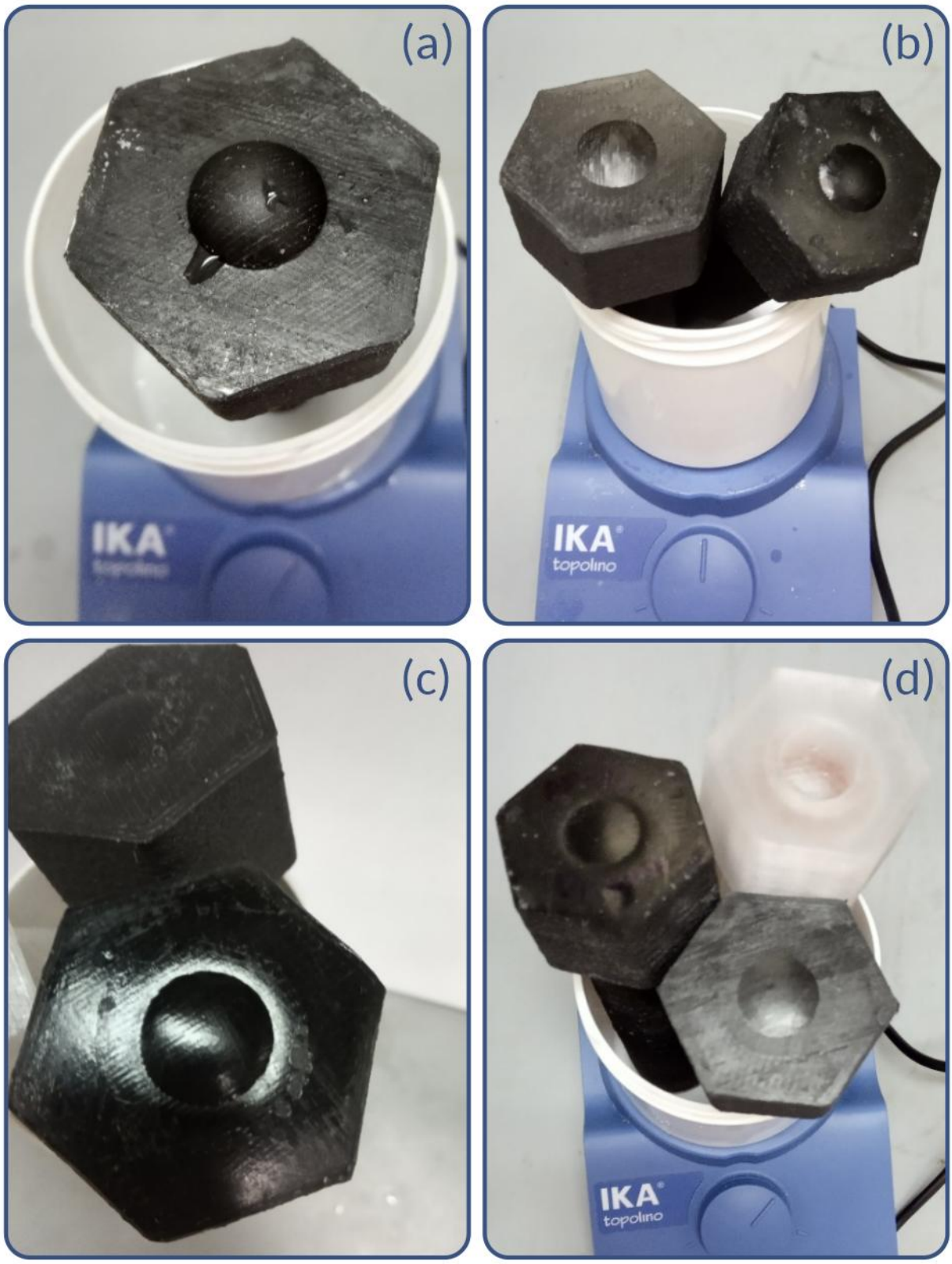

Figure S20. Rupture tests of bursting discs integrated into the base of the caps: (a) PA-CF using 9 mmol of Na_2CO_3; (b, c) PA-CF and PP-GF30 when exposed to > 5 mmol of reagents; (d) caps after hydrolysis of 4 mmol of CaC_2.

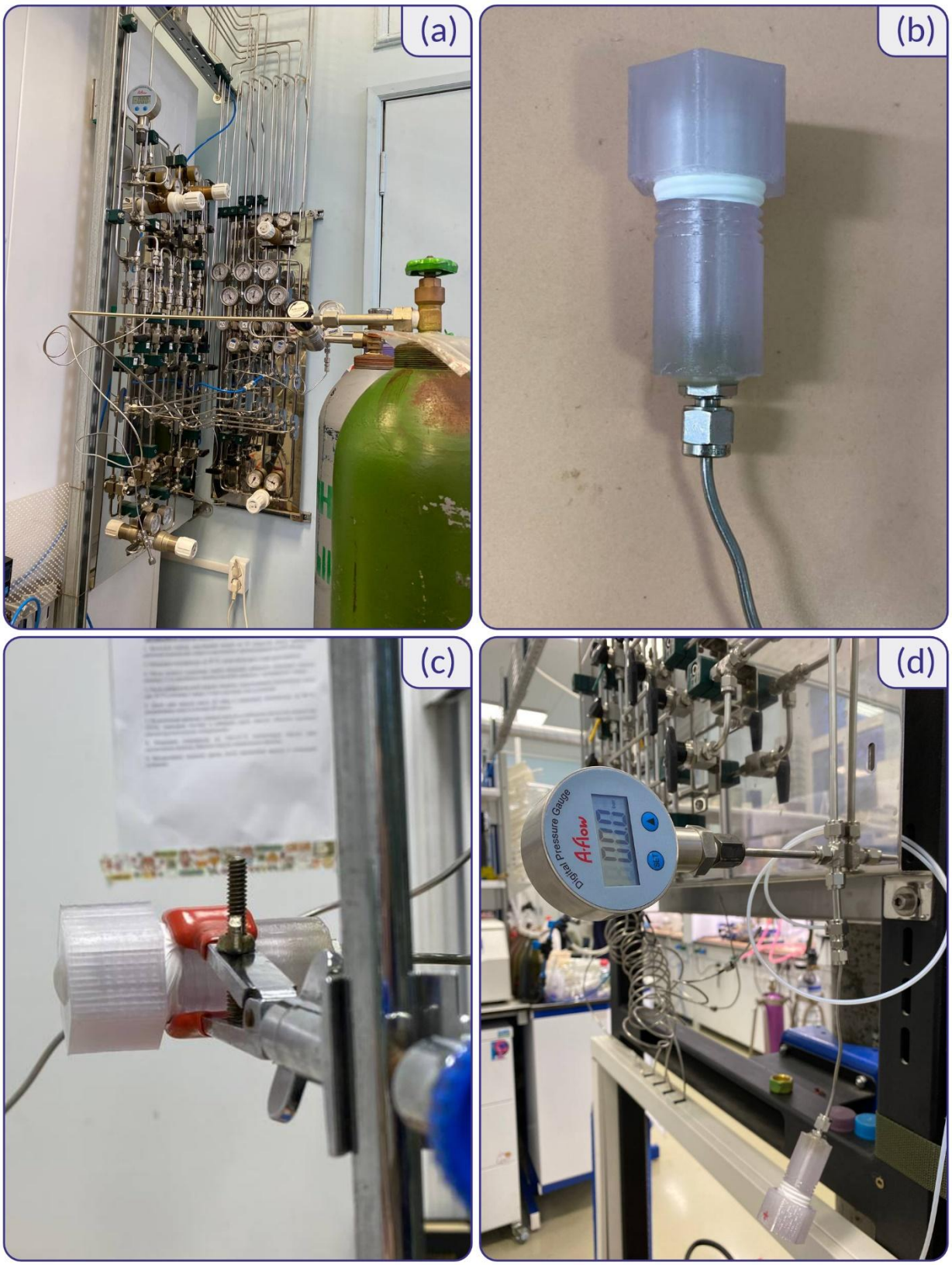

Figure S21. Testing of bursting discs with pure gases from cylinders: (a) gas system with gas cylinders, capillaries and electronic manometer for experiments with argon and hydrogen; (b) reactor with cap with bursting disc connected via adapter and capillary to gas system; (c) testing of bursting disc with pure hydrogen from gas cylinder; (d) gas system with electronic pressure gauge for experiments with helium.

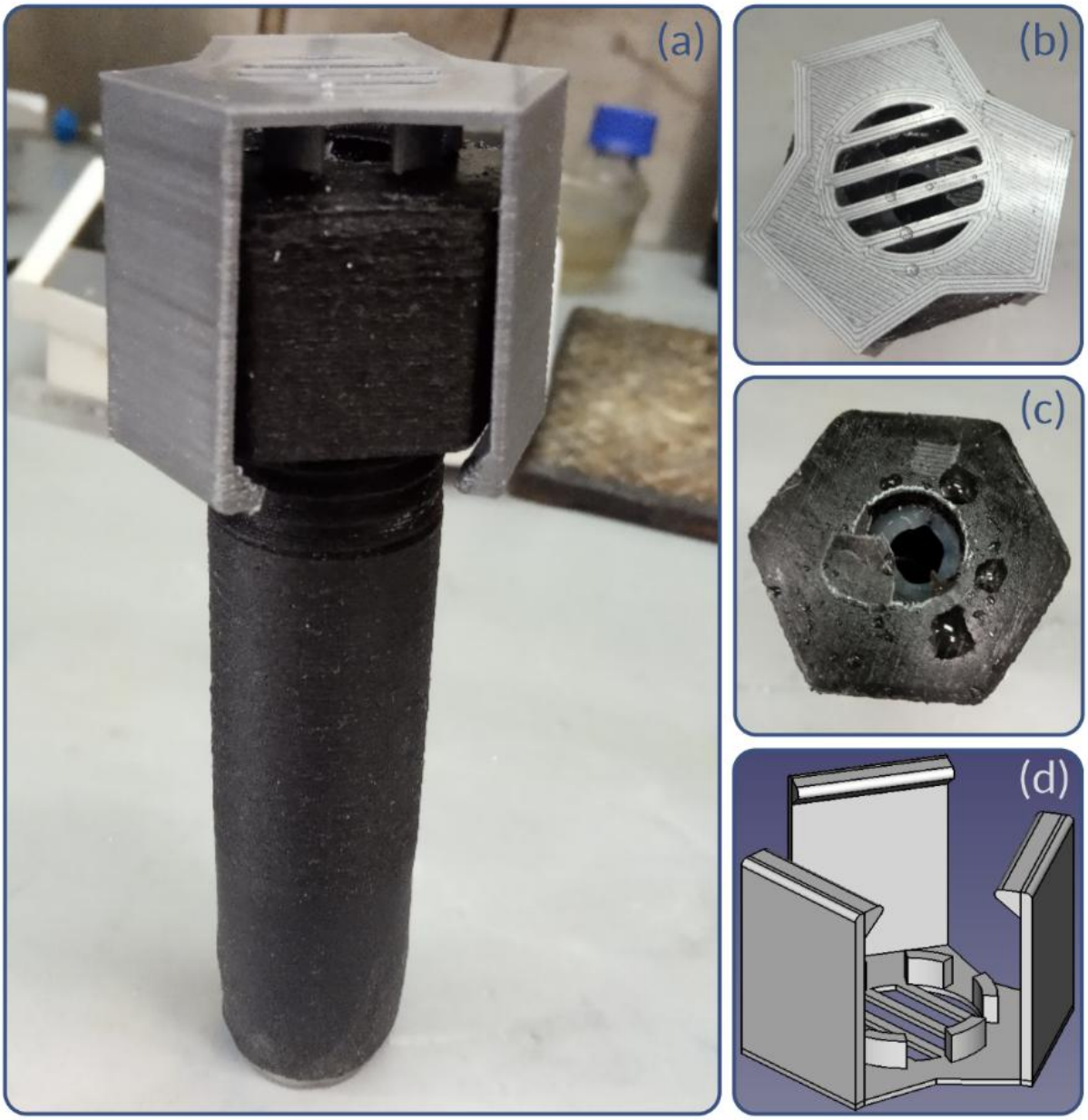

Figure S22. (a, b) I-tube reactor made of PP-GF30 before the experiment with a safety screen made of SBS plastic; (c) cap with a bursting disc after the experiment and removal of the safety screen; (d) 3D model of the safety screen.

A safety screen was developed to prevent uncontrolled ejection of the disc from the wall of the cap (Figure S19b). This screen is attached to the top of the cap (Figure S22), blocking the knockout of the disc when the pressure is critical. The safety screen was manufactured by the FFF method from styrene-butadiene-styrene (SBS).

To test the performance of the safety screen, an experiment was conducted by loading 8 mmol (848 mg) of Na_2CO_3 and 9 mmol (1.17 g) of citric acid. During the experiment, the screen proved to be effective and blocked the disc from "flying out" when the critical pressure reached the system during CO_2 generation.

2.3. Thermal conductivity of the FFF reactors

Table S5. Heating PETG and PP-GF30 I-tube type 2 reactors.

Warm-up time, min[a]	$T_{external}$, °C	$T_{internal}$, °C	
		PETG[c]	PP-GF30[d]
0	100	26	26
15-20	100	73-75	85
30-35	120	85	98
35-40	125	99	103
45	130	103	106
50	131	107	107
60	150	120	119
70	160	130	129
72	161	-	130
25-30[b]	125	100	-
20[b]	121	-	100
40-45[b]	160	130	-
40-45[b]	161	-	130

[a]The summarized time for heating the heat medium from the set value to the new set value and the time for attaining the plateau temperature inside the reactor are given; [b] the time to reach the set temperature is given without taking into account the time of thermostatization at intermediate stages; [c] a mercury thermometer is used for temperature control; [d] an electronic thermometer is used for temperature control.

Table S6. Data from the polyamide (PA-CF) reactor heating experiment.

Warm-up time, min [a]	$T_{external}$, °C[C]	$T_{internal}$, °C[C]
0	100	23
10	100	82
15	100	93
20	100	94
25	100	94
30	105	98
35	105	100
40	110	103
45	110	105
50	110	105
55	115	106
60	125	107
70	126	108
75	130	111
80	130	115
85	137	123
90	140	132
95	140	136
110	155	-
20-25[b]	105	100
40[b]	140	130

[a]The summarized time for heating the heat medium from the set value to the new set value and the time for attaining the plateau temperature inside the reactor are given; [b] the time to attain the set temperature is given without taking into account the time of thermostatisation at intermediate stages; [c] a mercury thermometer is used for temperature control.

Table S7. The results of the experiment on heating glass reaction tubes.

Warm-up time, min[a]	$T_{external}$, °C	$T_{internal}$, °C	
		Tube 10 ml[c]	Tube 50 ml[d]
0	100	23	23
5	100	90	96
10	100	94	98
15	100	94	98
20	100	98	100
21	100	100	100
30	130	125	129
34	130	126	130
50	135	130	-
20-21[b]	100	100	100
34[b]	130	-	130
50[b]	135	130	-

[a]The summarized time for heating the heat medium from the set value to the new set value and the time for attaining the plateau temperature inside the reactor; [b] final heating time to the set temperature; [c] a mercury thermometer is used for temperature control; [d] an electronic thermometer is used for temperature control.

2.4. Heat resistance tests of the FFF reactors

Figure S23. Plastic reactors after heating experiments: (a) PP-GF30 and PETG; (b) PA-CF; (c), (d) deformation of the inner surface of the PA-CF reactor; (e) PETG reactors after the heating experiment - exposure to chemical (left) and thermal (100 °C, right) factors

2.5. Strength tests of the FFF reactors under pressure

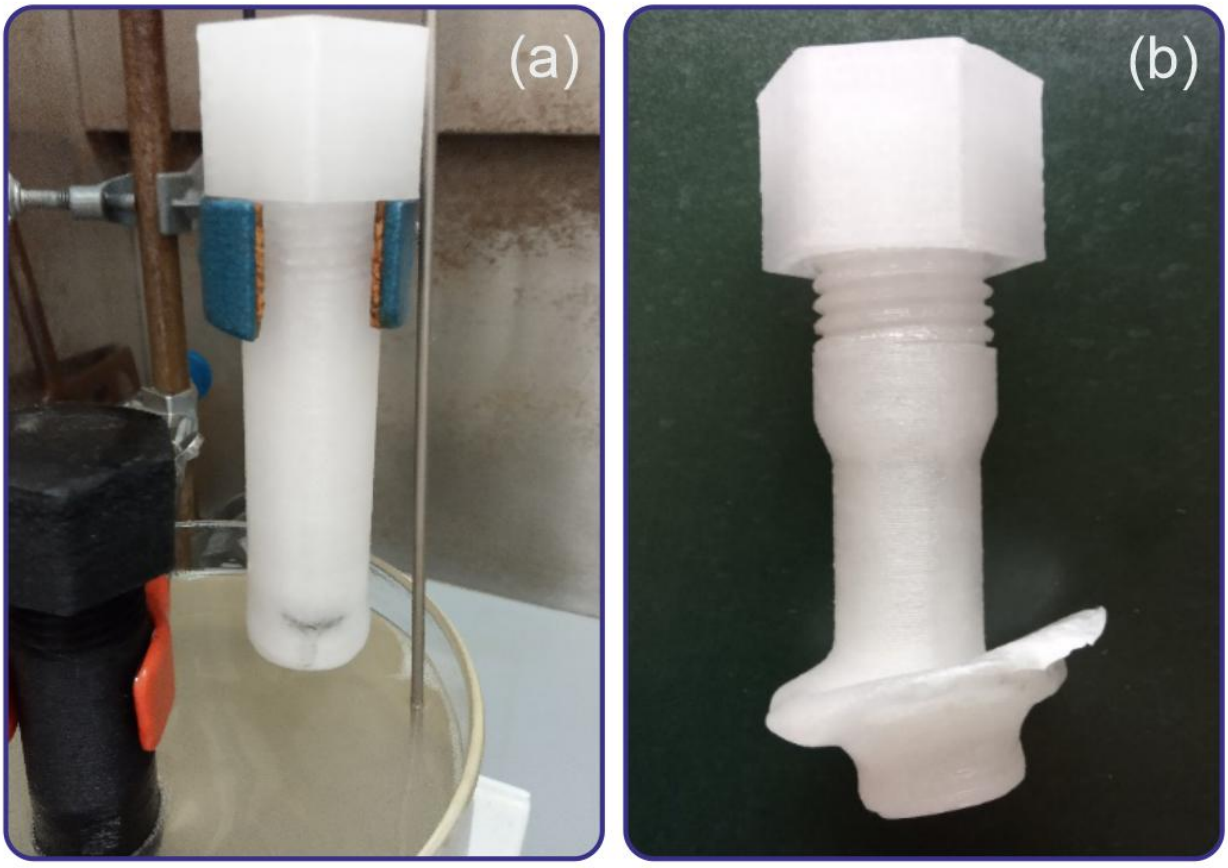

Figure S24. I-tube type 3 (a) and type 2 (b) reactors made of PETG after an experiment with 3 mmol calcium carbide hydrolysis.

3. Experimental details for manufacturing and testing the high-pressure reactors

3.1. 3D printing of the reactors by the FFF method

In this work, the materials chosen for FFF 3D printing were polyethylene terephthalate glycol (PETG), polypropylene filled with 30 % glass fiber (PP-GF30), and polyamide filled with 20 % carbon fiber (PA-CF).

In the first stage, the reactor design was developed (the optimal thread size, wall thickness, and possibility of providing impermeability were selected). PETG was used for this application, which was chosen as an example of a general material due to its availability and ease of use in FFF printing.

Previously, it was shown that filled polymers are promising structural materials for manufacturing batch reactors and flow reactors.[1] Carbon fiber-filled polyamide and glass fiber-filled polypropylene showed high stability in various organic solvents both at room temperature and when heated. In the present work, these materials were selected for the FFF manufacturing of high-pressure plastic reactors.

All FFF reactors were manufactured using the FFF method with a Picaso Designer X-Pro desktop 3D printer (Figure S25). This printer is a personal desktop 3D printer with the specifications shown in Table S7.

Table S8. Picaso Designer X-Pro technical data.

Number of extruders	1
Number of nozzles	2
Printing area	201 x 201 x 210 mm
Minimum layer thickness	10 microns (0.01 mm)
Plastic filament diameter	1.75 mm
Nozzle diameter	0.2 - 0.8 mm
Maximum extruder temperature	410 °C
Maximum table temperature	150 °C

This 3D printer uses a wide range of general purpose and engineering thermoplastics, such as ABS, PLA, HIPS, PVA, ASA, PET, PC, PETG, SBS, PMMA, TPU, PA, and SEBS, as well as composites based on them. The Picaso Designer X-Pro is characterized by high kinematic precision that allows the printing of a functional metric thread, including small sizes for safety modules. The ability to print such functional parts is especially important for this project.

It should be noted that during this project, the printing of caps with bursting discs was performed one by one in the same place on the bed to maximize the reproducibility of the mechanical characteristics of the bursting discs.

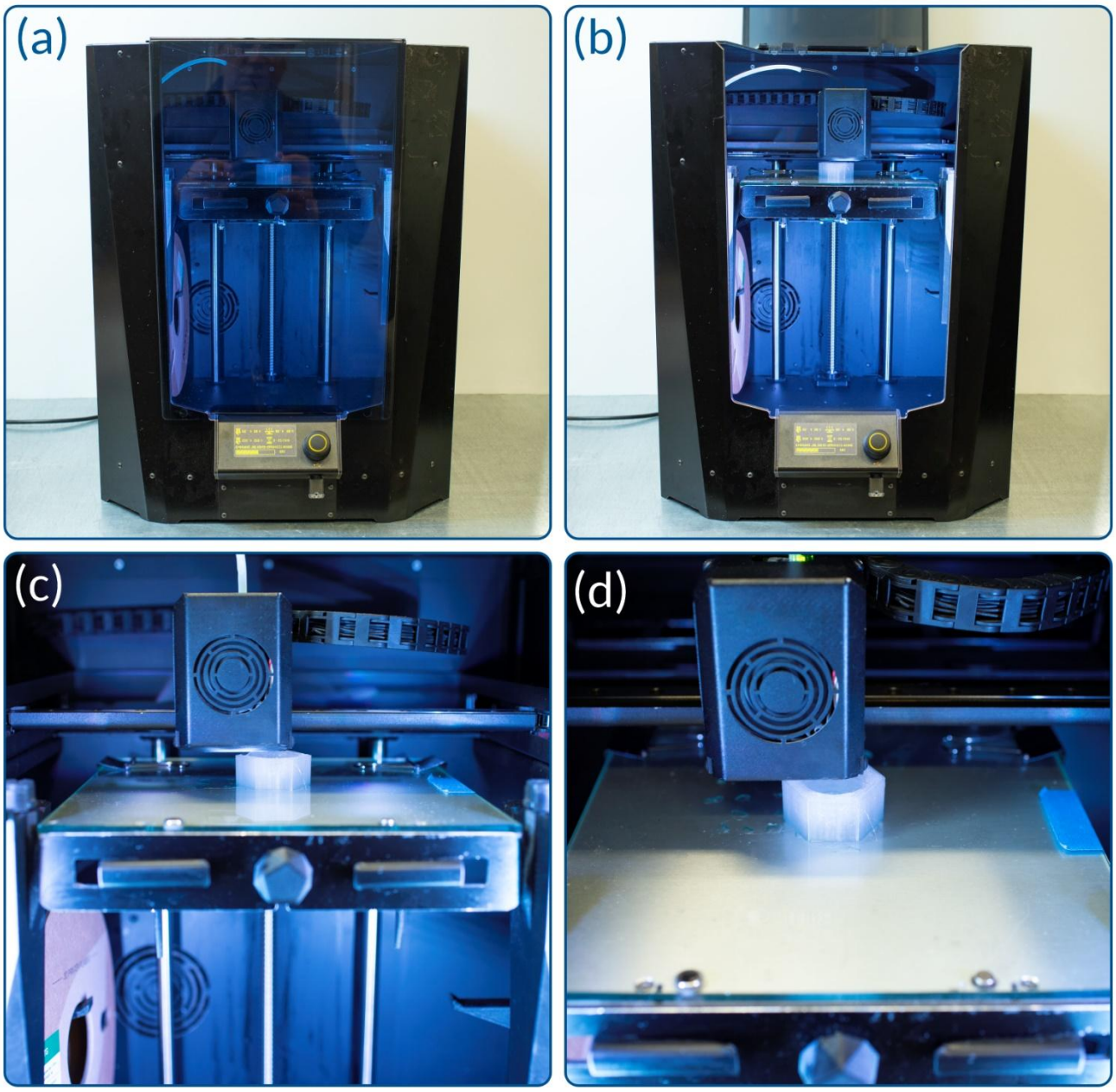

Figure S25. Manufacturing of the reactor cap with a rupture disc by PETG using the Picaso Designer X-Pro printer: (a) printer with a closed chamber; (b) printer with an open chamber; (c) printer bed with a printed cap, side view; (c) printer bed with a printed cap, top view.

FFF reactors were printed using a 0.5 mm diameter steel nozzle. The internal filling density of the samples is 100 %. The extrusion width (w) and k-value varied depending on the material and reactor type. More detailed printing parameters are shown in Table S7. The G-code was generated by the Polygon X program, which is natively associated with Picaso 3D printers.

Table S9. Reactor printing parameters.

Parameters	PETG	PP-GF	PA-CF
Drying plastic before printing	yes	yes	yes
Drying temperature, °C	60	60	80
Drying time (minimum), h	1	2	5
Printing in a closed chamber	no	no	yes
Printing on a substrate	no	yes	no
Printing on thick glue	no	no	yes
Spray adhesive printing	yes	no	no
Tube-stundart (5 mm)			
Parameters	PETG	PP-GF	PA6-CF
Extruder Diameter, mm	0.5	0.5	0.5
Extruder Width, mm	0.65	0.62	0.62
Extrusion Multiplier	0.98	1.00	0.98
Extruder Use Retract	1	1	1
Layer Height	0.25	0.25	0.25
Temperature Extruder 1, °C	240	240	260
Heated Bed, °C	90	80	100
Brim	yes	yes	yes
Build time	2 hours 33 minutes	3 hours 1 minutes	3 hours 1 minutes
Thin-wall-tube (3 mm)			
Parameters	PETG	PP-GF	PA-CF
Extruder Diameter, mm	0.5	0.5	0.5
Extruder Width, mm	0.65	0.62	0.62
Extrusion Multiplier	1.1	1.15	0.98
Extruder Use Retract	1	1	1
Layer Height	0.25	0.35	0.25
Temperature Extruder 1, °C	265	290	250
Heated Bed, °C	110	60	110
Brim	yes	yes	yes
Build time	2 hours 33 minutes	1 hour 36 minutes	2 hours 13 minutes
Plastic volume, mm^3	-	33907.04	27752.91
Plastic weight, g	-	42.38	34.69
Large-volume-tube (100 ml)			
Parameters	PETG	PP-GF	PA-CF
Extruder Diameter, mm	0.5	0.5	0.5
Extruder Width, mm	0.65	0.64	0.63
Extrusion Multiplier	1.06	1.05	0.98
Extruder Use Retract	1	1	1
Layer Height	0.25	0.25	0.25
Temperature Extruder 1, °C	236	240	250
Heated Bed, °C	95	50	110
Brim	yes	yes	yes
Build time	6 hours 7 minutes	6 hours 11 minutes	6 hours 15 minutes
Plastic volume, mm^3	116701.77	115063.77	107024.85

Plastic weight, g	145.88	143.83	133.78
Y-tube			
Parameters	**PETG**	**PP-GF**	**PA-CF**
Extruder Diameter, mm	0.5	0.5	0.5
Extruder Width, mm	0.64	0.62	0.63
Extrusion Multiplier	1.06	1.04	0.99
Extruder Use Retract	1	1	1
Layer Height	0.25	0.25	0.25
Temperature Extruder 1, °C	236	240	250
Heated Bed, °C	70	50	110
Brim	yes	yes	yes
Build time	4 hours 38 minutes	4 hours 44 minutes	4 hours 41 minutes
Plastic volume, mm^3	75002.28	73036.10	69816.29
Plastic weight, g	93.75	91.30	87.27
H-tube			
Parameters	**PETG**	**PP-GF**	**PA-CF**
Extruder Diameter, mm	0.5	0.5	0.5
Extruder Width, mm	0.64	0.65	0.64
Extrusion Multiplier	1.06	1.05	1.05
Extruder Use Retract	1	1	1
Layer Height	0.25	0.25	0.25
Temperature Extruder 1, °C	236	240	250
Heated Bed, °C	80	50	110
Brim	yes	yes	yes
Build time	4 hours 18 minutes	4 hours 8 minutes	4 hours 12 minutes
Plastic volume, mm^3	77531.71	74543.93	74274.72
Plastic weight, g	96.91	93.18	92.84

3.3. Heating of the reactors in a liquid medium

The heating of Type I reactors using DMSO was performed in a silicone bath at 130-150 °C with 3 mL of solvent. During the experiments, it was found that the heating of DMSO in the inner volume of the reactor made of PP-GF30 to a given temperature occurred when the temperature difference between the heat carrier and the solvent in the internal volume remained within 30-40 °C.

The experiment of heating the reactor made of PETG with DMSO in the internal volume of the reactor was carried out at the temperature of the heat carrier at 145 °C. At the same time, the temperature of the solvent reached approximately 100 °C. When the temperature of the heat carrier was increased to 150 °C, the temperature of the solvent inside the reactor increased to 110 °C, and when the external temperature was increased to 155 °C, the temperature of the DMSO was 130 °C. It should be noted that the heating of the solvent in the PETG reactor was faster than that in the PP-GF30 reactor. In addition, the part of the PETG FFF reactor immersed in the silicone bath was deformed, softened and swollen under the action of the organic solvent and elevated temperature.

3.4. Solvent heating experiments in FFF reactors

In the test reactor, which was equipped with a magnetic stir bar and thermometer, 3 mL of DMSO was added, after which the vessel was immersed in a silicone bath preheated to 100 °C on a magnetic stirrer. For uniform heating, a part of the reactor with solvent was completely immersed in the heat carrier. The heating time started from the moment the reactor was placed into the heat carrier. The maximum achievable temperature inside the reactor at a given heat carrier temperature was considered to be the value maintained for 10 minutes or more with a maximum deviation of no more than 0.5 °C. If the temperature inside the reactor was lower than the desired temperature, a new higher heat carrier temperature was set. The temperature rise inside the reactor was monitored, and its value was recorded using electronic and mercury-in-glass thermometers. This experiment was repeated until the DMSO temperature inside the reactor reached the desired temperature of 100 or 130 °C.

3.5. Pressure test of FFF reactors with acetylene

3 mL of DMSO and calculated amounts of calcium carbide and water (molar ratio CaC_2:H_2O = 1:2) were placed in a reactor equipped with a magnetic stir bar. After adding water, the reactor was sealed with a cap, placed in a preheated silicone bath and kept for up to 20 min. If the reactor did not deform after 20-30 min, the experiment with this calcium carbide loading was completed and repeated with a larger amount of carbide.

To achieve an internal temperature of 100 °C when testing the PETG FFF reactor, the bath heat carrier temperature was 125 °C (the reactor could not withstand higher temperatures). For the PP-GF30 reactors, the heat carrier temperature was increased to 150 °C to provide an internal reactor temperature of 130 °C.

The pressure of the formed acetylene was calculated by the following equation:

$$V(C_2H_2) = n \times V_m;$$

$$P = \frac{V(C_2H_2)}{V_{reactor}},$$

where $V(C_2H_2)$ is the volume of acetylene produced (mL), $V_{reactor}$ is the reactor volume (mL), n is the amount of calcium carbide taken to produce acetylene (mmol), V_m is the molar volume (22.4 l/mol), P is the pressure (atm.).

3.6. Bursting discs testing using compressed air

The rupture of bursting discs at critical pressure depends on the material from which the discs are made. In particular, PETG discs with a diameter of 15 mm and thickness of 0.07 mm were characterized by destruction "along the lines" of plastic. With the gradual injection of air to create overpressure in the system, slight swelling of the disc was observed. When the overpressure reached approximately 2 bar, the disc lost its impermeability with the formation of a through hole between the plastic lines formed by the nozzle during printing (the disc thickness was one layer). The discs with a diameter of 15 mm and a thickness of 0.1 mm gradually inflate during plastic deformation when overpressure is applied to the system. The disc bursting occurs at a pressure of approximately 5 bar (Figure S17).

PP-GF30 discs with a diameter of 15 mm and a thickness of 0.05 mm are impermeable at a pressure of 1 bar. A pressure of 2 bar results in a crack along the FFF raster lines. The discs with a

diameter of 15 mm and thickness of 0.07 mm at a pressure of 6-7 bar were completely separated from the wall of the cap and ejected by the air flow as a separate part.

A disc with a diameter of 15 mm and thickness of 0.1 mm does not lose its impermeability at a pressure of 7.5 bar, which is the limit pressure created by the compressor. PA-CF discs with a diameter of 15 mm and a thickness of 0.07 mm were slightly inflated and irreversibly deformed at an ultimate system pressure of approximately 3 bar. The discs with a diameter of 15 mm and thickness of 0.1 mm deformed at a pressure of approximately 7.5 bar, but there was no bursting of the disc.

3.7. Bursting discs test using C_2H_2

The diameter of the bursting discs integrated into the caps was 15 mm, and the thicknesses were 0.05, 0.07, and 0.1 mm for the PP-GF30 cap and 0.07 and 0.1 mm for the PA-CF and PETG caps, respectively.

3 mL of DMSO and the calculated amount of CaC_2 were placed in a reactor equipped with a magnetic stir bar. Then, a double excess of water relative to carbide was added, and the mixture was immediately closed with a cap with a disc. A ½" silicone gasket was used to seal the splice. The mixture was stirred at room temperature until the disc burst, and if the disc did not burst, the experiment was terminated after 15-20 minutes of chemical reaction.

3.8. Bursting discs test using CO_2

The calculated stoichiometric amounts of sodium carbonate and citric acid were placed in a reactor equipped with a magnetic stir bar. The dry mixture was separated by a fine filter, on which a plastic cylinder with 3 mL of water was placed (Figure S18). The reactor was closed with a cap, and the joint was previously sealed with a silicone gasket. Then, the liquid (water) and solid (sodium carbonate, citric acid) phases were mixed and placed on a magnetic stirrer. The reaction mixture was stirred at room temperature until the bursting of the disc integrated into the wall of the cap. When the disc was stable for 15 minutes, the experiment was terminated.

3.9. Preparation of vinyl derivatives of steroids

Reduction of progesterone

To a solution of 1.0 g (3.18 mmol) of progesterone **1** in 20 mL of dry THF at room temperature was added 181 mg (4.77 mmol) of $NaBH_4$ (Scheme S2). The reaction course was controlled by TLC. The unhealthy hydride was decomposed by the addition of 10 mL of distilled water. The mixture was extracted with EtOAc (2 × 50 mL) and washed with brine (2 × 30 mL), and the organic layer was drained over Na_2SO_4. White powder, yield of **2** – 98%.

^{1}H NMR (400 MHz, $CDCl_3$, δ, ppm): 5.17 (s, 1H), 4.09–3.98 (m, 1H), 3.61 (td, J = 12.2, 6.1 Hz, 1H), 3.37 (s, 1H), 2.18–2.03 (m, 1H), 2.02–1.87 (m, 2H), 1.86–1.78 (m, 1H), 1.68–1.50 (m, 4H), 1.44–1.30 (m, 3H), 1.29–1.14 (m, 3H), 1.15–1.01 (m, 4H), 1.03 (d, J = 6.1 Hz, 3H), 0.95 (s, 3H), 0.82–0.76 (m, 1H), 0.68 (s, 3H). The spectral data are consistent with the literature.[2]

*Synthesis of 20-vinyloxy-20-methylpregnene-3-ol **3***

Alcohol **2** (50 mg, 0.16 mmol), calcium carbide (192 mg, 3 mmol), potassium fluoride (0.5 g, 9 mmol), potassium hydroxide (272 mg, 4 mmol) and water (0.1 ml, 6 mmol) were added to a reaction PP-CF tube with 3 mL of DMSO. The tube was sealed, and the mixture was heated at

150°C for 5 h with vigorous stirring. After cooling to 25 °C, the mixture was filtered, extracted with Et_2O (3 × 10 mL), and treated with brine (3 × 10 mL), after which the organic layer was dried over Na_2SO_4. The solvent was removed at reduced pressure, and the residue was chromatographed on neutralized triethylamine silica gel (eluent – hexan:Et_2O = 50:1, visualizer – 5% $KMnO_4$). Brown oil, yield – 57%. ^{1}H NMR (400 MHz, $CDCl_3$) δ 6.37 (dd, J = 14.2, 6.6 Hz, 1H, H-22, CH=CH2), 5.33 (d, J = 1.3 Hz, 1H, H-4), 4.31 (dd, J = 14.2, 1.4 Hz, 1H, H-23A), 4.35–4.27 (m, 1H, H-3), 4.01 (dd, J = 6.6, 1.4 Hz, 1H), 3.73 (tt, J = 11.4, 5.7 Hz, 1H), 2.27–2.15 (m, 1H), 2.10 – 1.99 (m, 3H), 1.79–1.69 (m, 2H), 1.69–1.57 (m, 4H), 1.52–1.40 (m, 2H), 1.37 (dd, J = 12.9, 3.5 Hz, 1H), 1.33–1.22 (m, 4H), 1.19–1.09 (m, 2H), 1.13 (d, J = 6.1 Hz, 3H), 1.06 (s, 3H), 1.02–0.97 (m, 1H), 0.91–0.85 (m, 1H), 0.77 (s, 3H), 0.81–0.71 (m, 1H). ^{13}C NMR (101 MHz, $CDCl_3$) δ 150.4 (CH=CH2), 149.0 (C), 119.4 (CH), 88.3 ($CH=CH_2$), 77.2 (C), 75.2 (CH), 70.5 (CH), 58.5 (CH), 55.6 (CH), 54.5 (CH), 42.4 (C), 39.9 (CH_2), 37.5 (C), 35.8 (CH_2), 35.1 (CH_2), 33.1 (CH_2), 32.2 (CH_2), 25.6 (CH_2), 24.5 (CH_2), 23.6 (CH_3), 20.9 (CH_2), 18.8 (CH_3), 12.5 (CH_3). HRMS (ESI): *m/z* calcd. for $C_{23}H_{36}O_2Ag^+$: 451.1761 [M+Ag]$^+$; found: 451.1756.

4. Application of FFF reactors in organic synthesis

4.1. Single-chamber FFF reactors for organic synthesis

S-vinylation

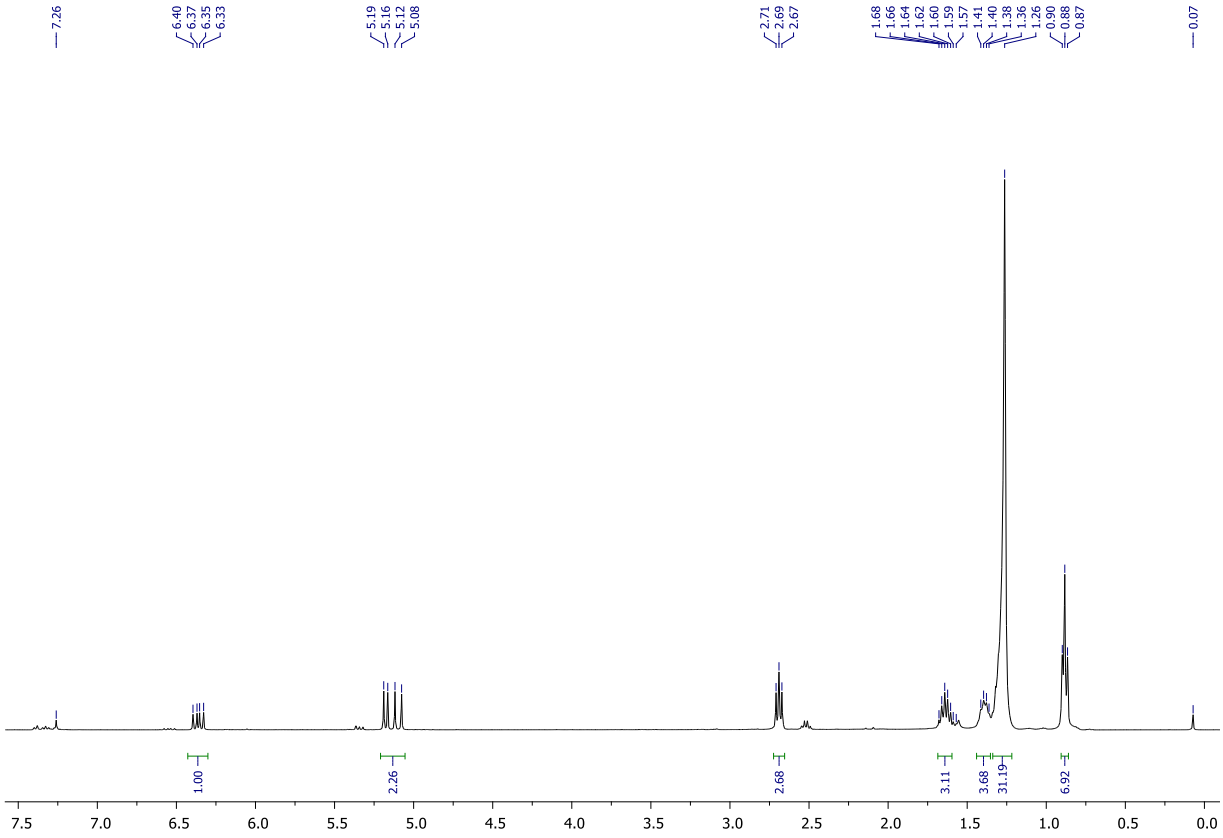

Figure S26. ^{1}H NMR spectrum (400 MHz, $CDCl_3$, δ, ppm) of the reaction mixture after vinylation of dodecanthiol. The synthesis was carried out in a reactor made of PP-GF30.

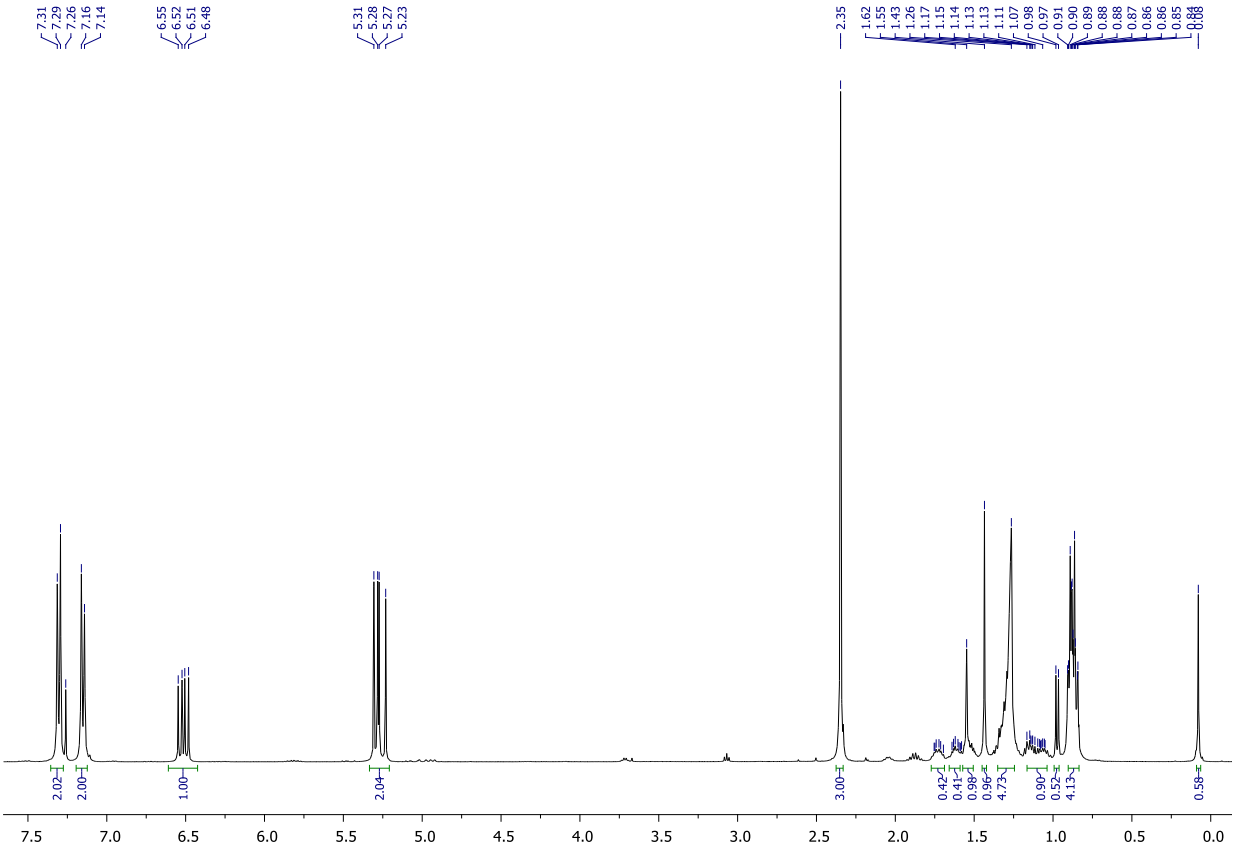

Figure S27. ^{1}H NMR spectrum (400 MHz, $CDCl_3$, δ, ppm) of the reaction mixture after vinylation of thiocresol. There are peaks of extraneous substances in the strong field. Probably, under the action of high temperature, the substances absorbed in earlier experiments are released into the reaction mixture. The synthesis was carried out in a reactor made of PP-GF30.

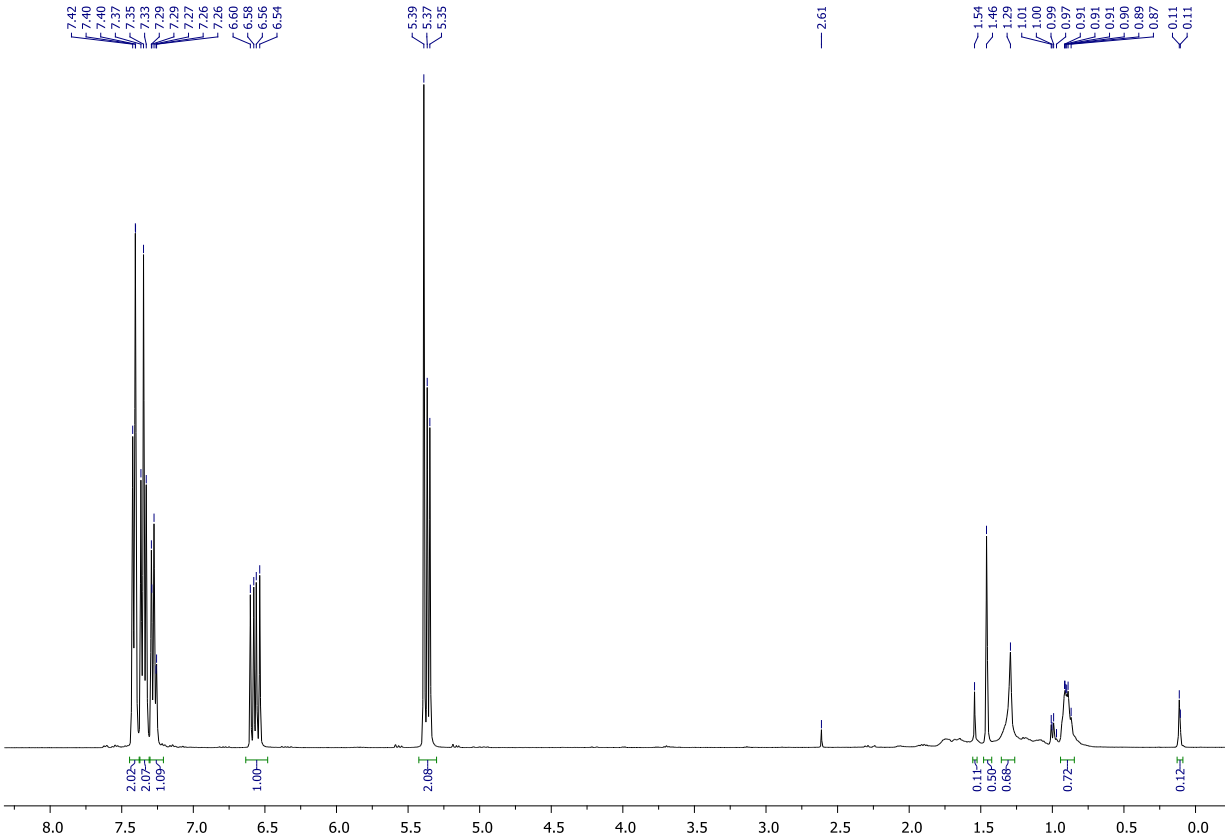

Figure S28. ^{1}H NMR spectrum (400 MHz, $CDCl_3$, δ, ppm) of the reaction mixture after vinylation of thiophenol in a scaled reaction. The product was not further purified (corrected for the presence of solvent). The synthesis was carried out in a reactor made of PP-GF30, and the reactor volume was 100 mL.

O-vinylation

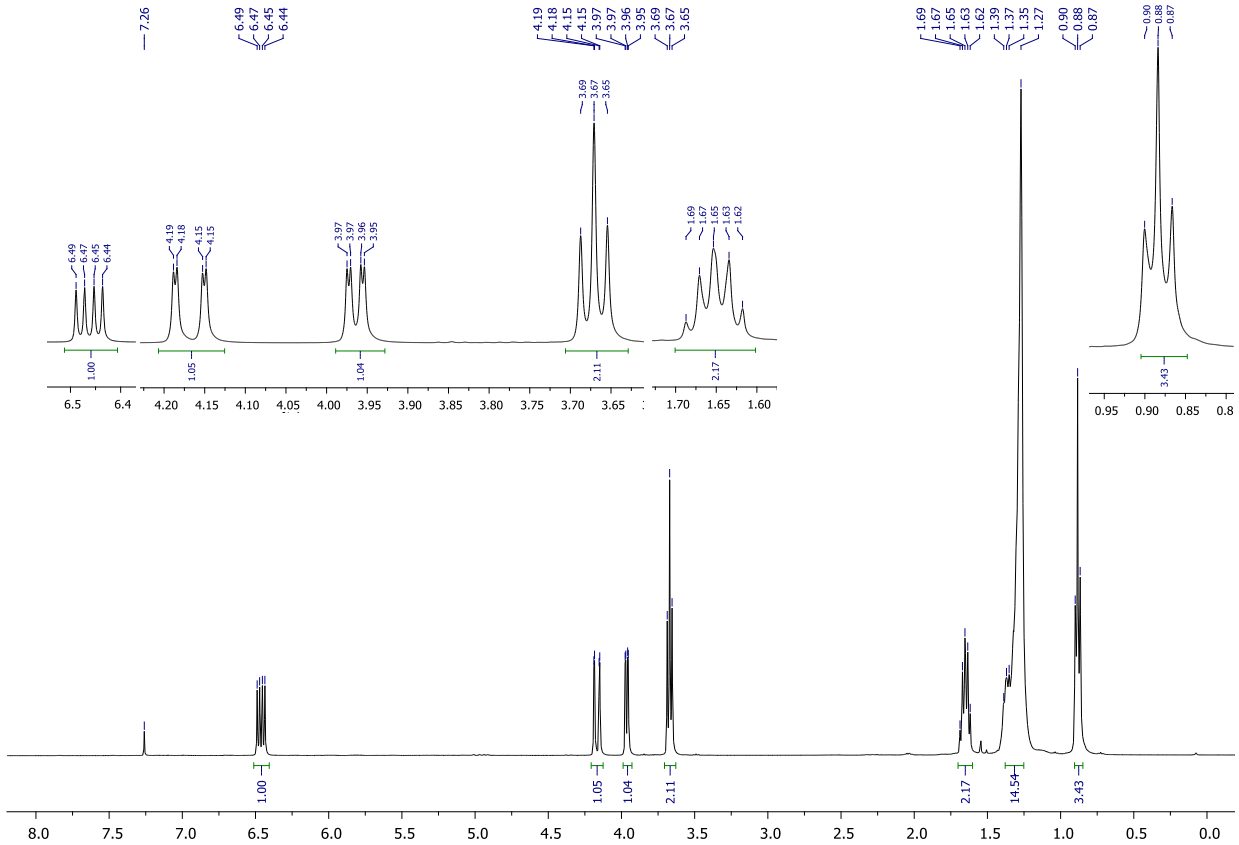

Figure S29. ^{1}H NMR spectrum (400 MHz, $CDCl_3$, δ, ppm) of decylvinyl ether obtained after the vinylation of decanol. The synthesis was carried out in a reactor made of PP-GF30.

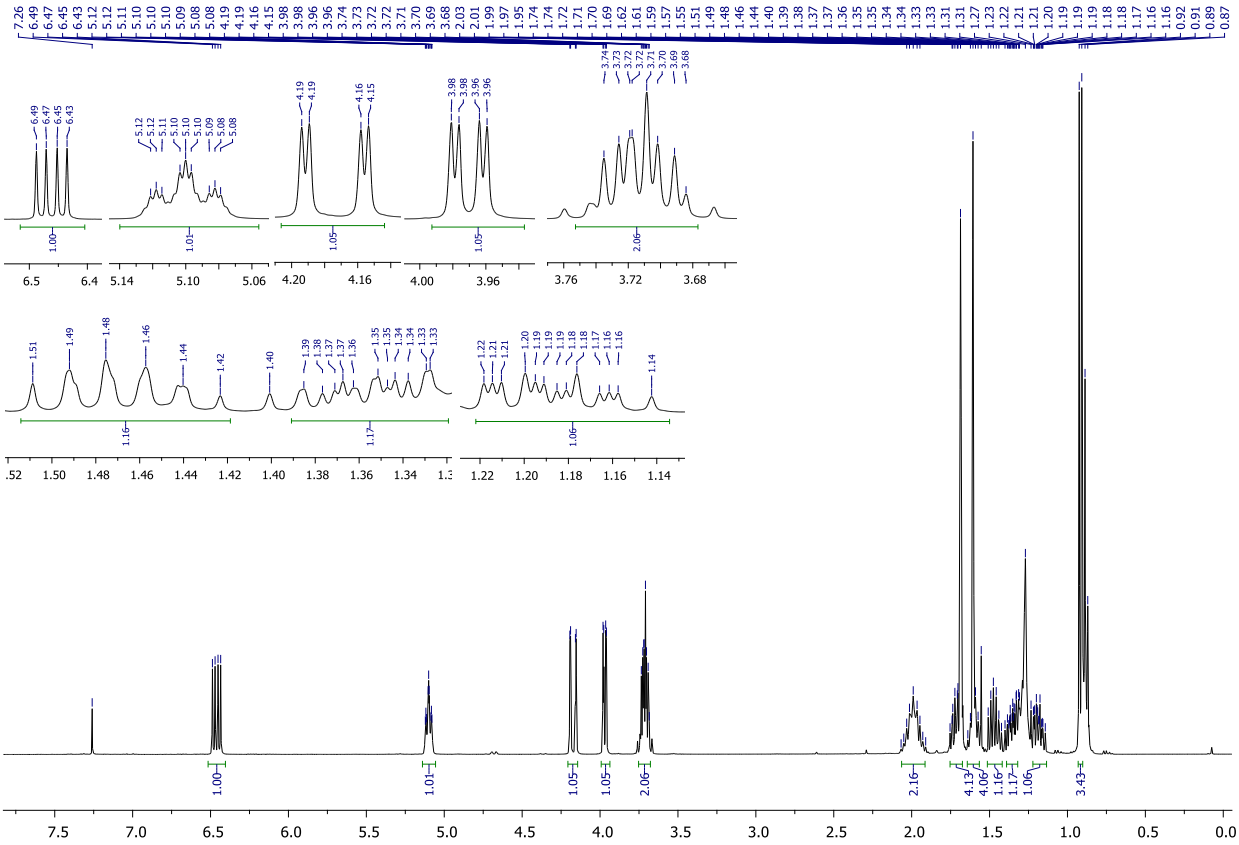

Figure S30. ^{1}H NMR spectrum (400 MHz, $CDCl_3$, δ, ppm) of citronellyl vinyl ester obtained after the citronellol vinylation reaction. The synthesis was carried out in a reactor made of PP-GF30.

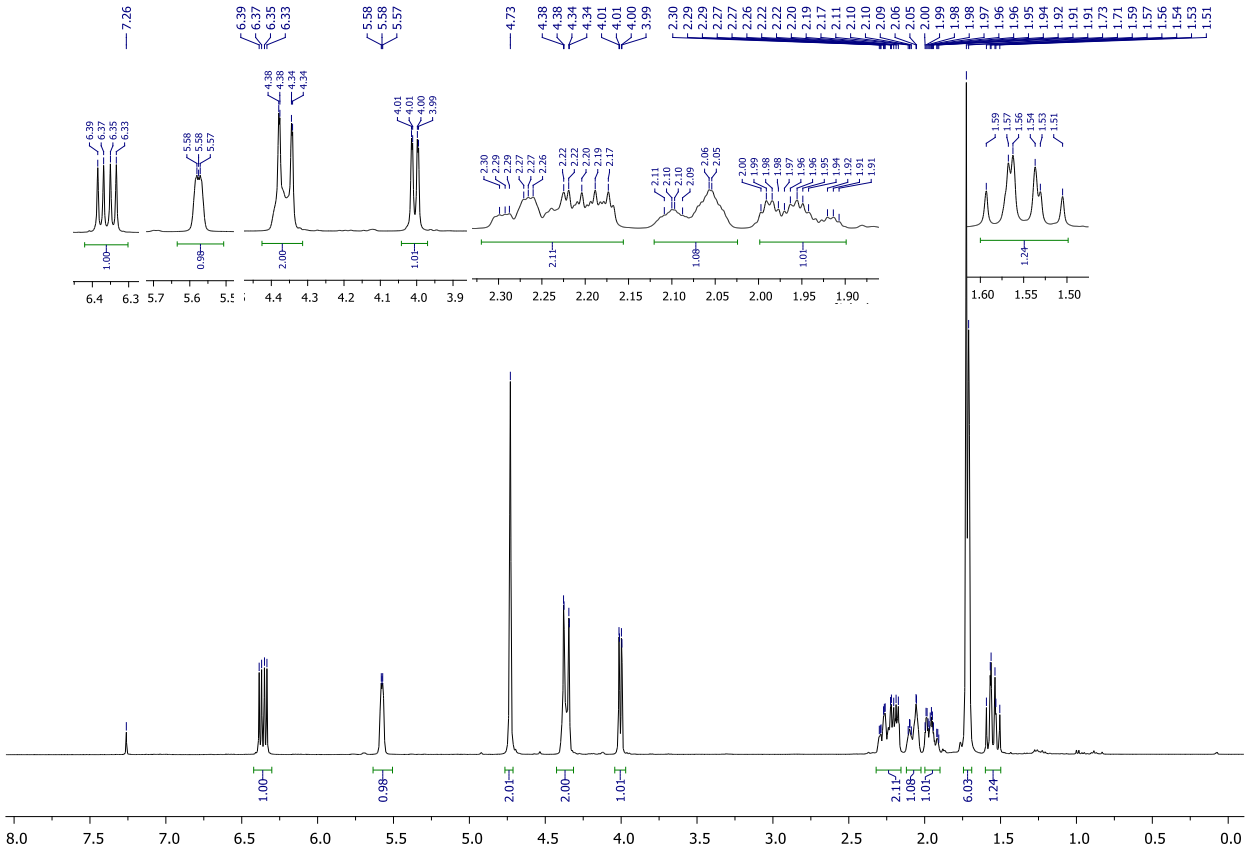

Figure S31. ^{1}H NMR spectrum (400 MHz, $CDCl_3$, δ, ppm) of the reaction mixture after vinylation of carveol. Conversion of alcohol amounted to 68%. The synthesis was carried out in a reactor made of PP-GF30.

N-vinylation

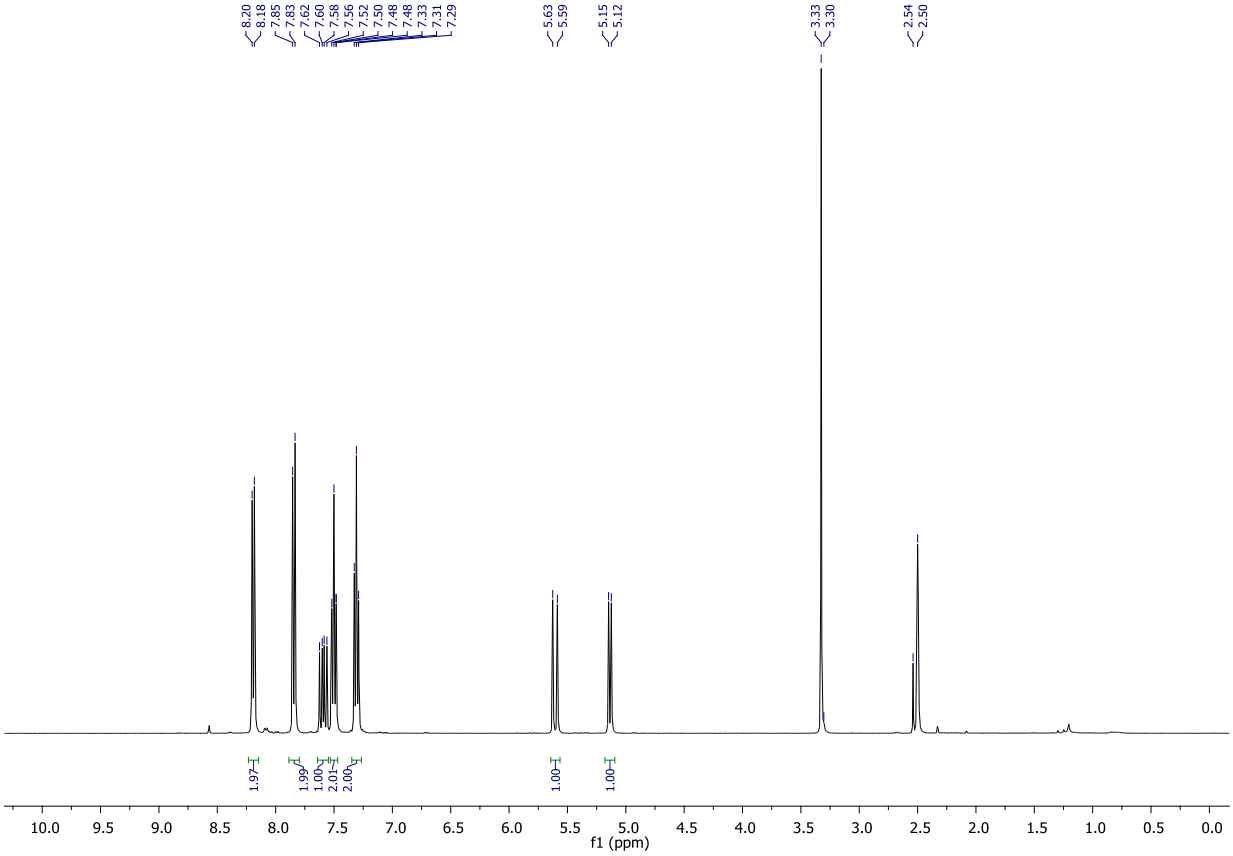

Figure S32. ^{1}H NMR spectrum (400 MHz, DMSO-d_6, δ, ppm) of vinylcarbazole after the carbazole vinylation reaction. The synthesis was carried out in a reactor made of PP-GF30.

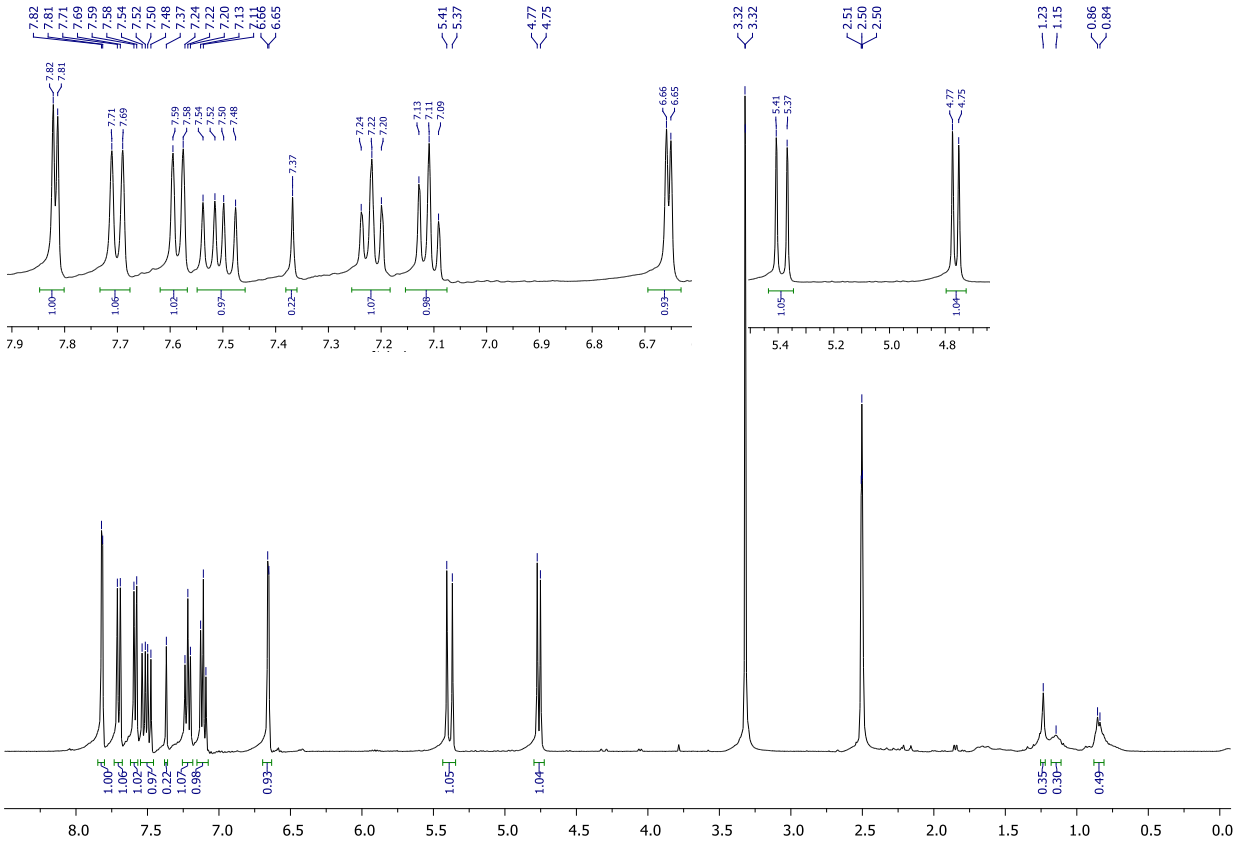

Figure S33. ^{1}H NMR spectrum (400 MHz, DMSO-d_6, δ, ppm) of vinylindole after the indole vinylation reaction. The synthesis was carried out in a reactor made of PP-GF30.

4.2. Double-chamber FFF reactors in organic synthesis

Cu-catalyzed click-reaction

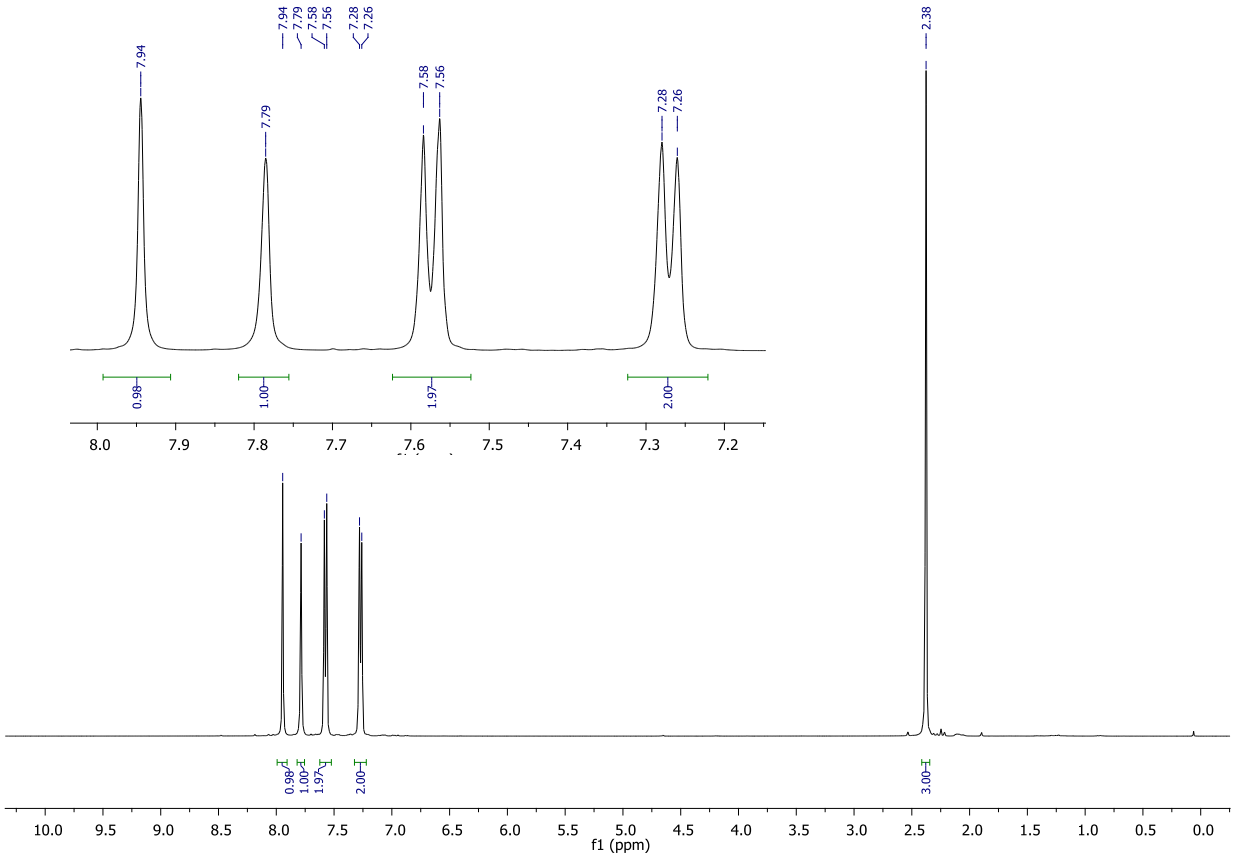

Figure S34. ^{1}H NMR spectrum (400 MHz, $CDCl_3$, δ, ppm) of 4-methylphenyl-1,2,3-triazole.

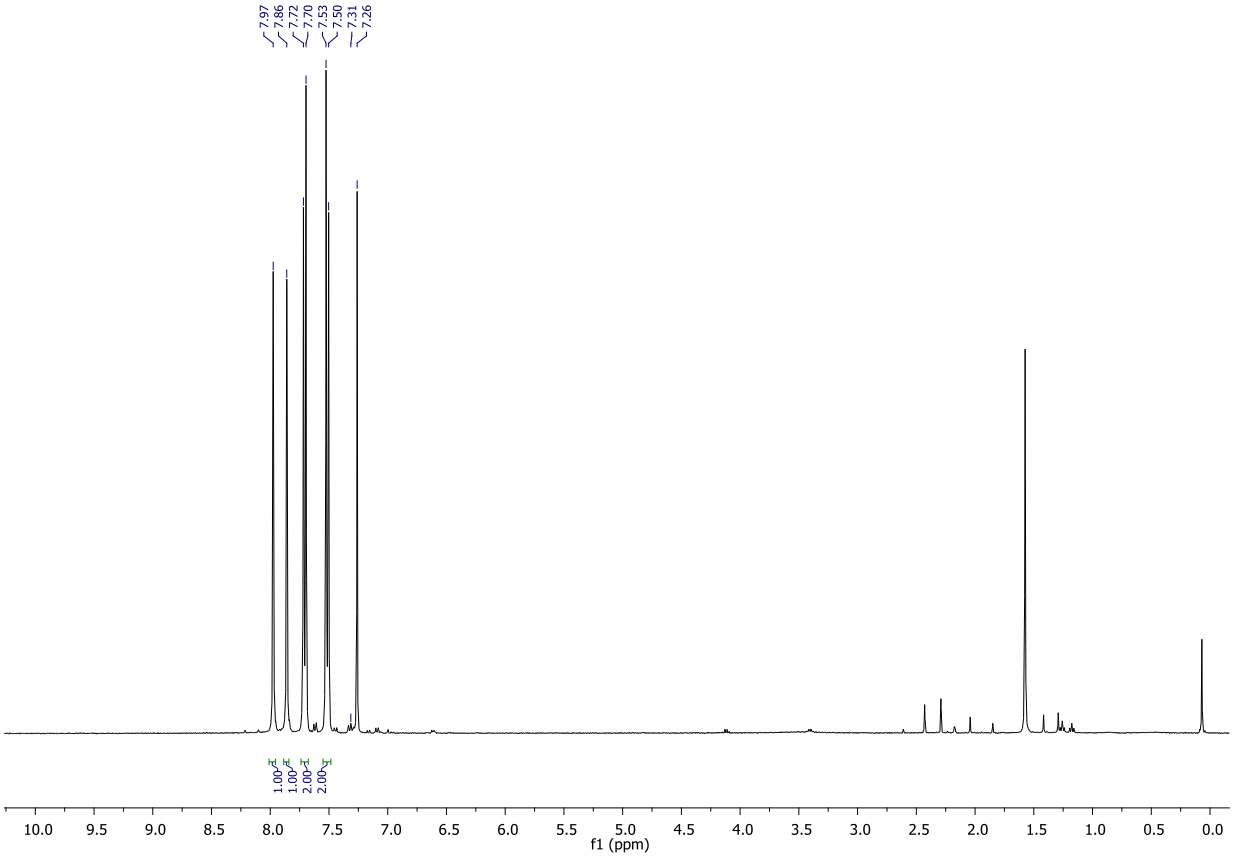

Figure S35. ^{1}H NMR spectrum (400 MHz, $CDCl_3$, δ, ppm) of 4-chlorophenyltriazole (reaction mixture).

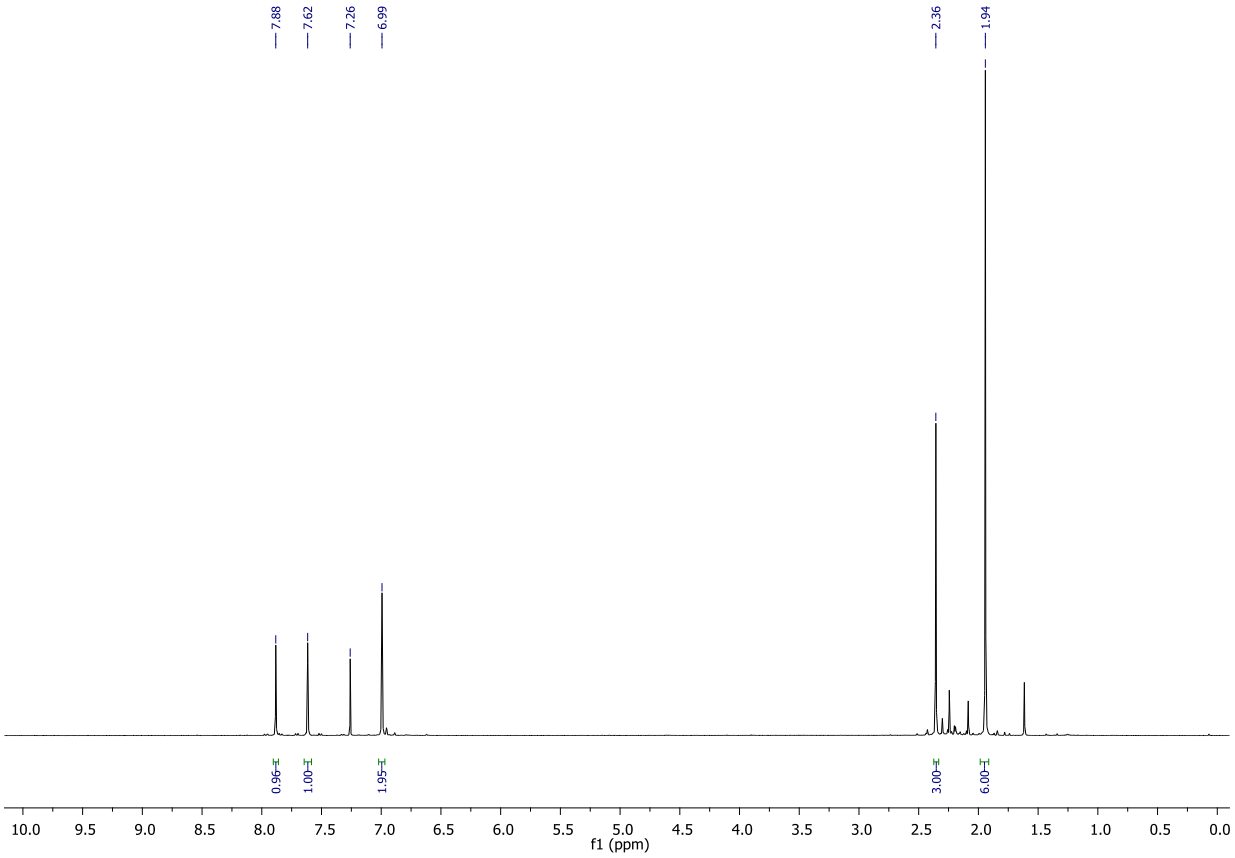

Figure S36. ^{1}H NMR spectrum (400 MHz, $CDCl_3$, δ, ppm) of mesityl-1,2,3-triazole (reaction mixture).

Preparation of vinyl derivatives of steroids

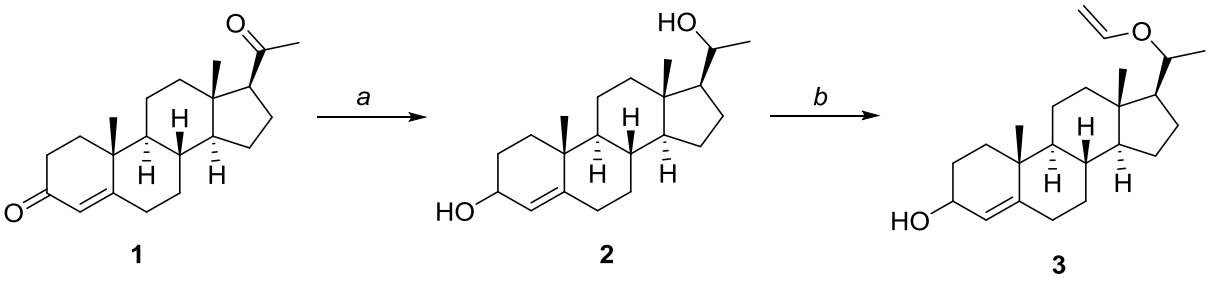

1 **2** **3**

a- 1 mmol of substrate **1**, 1.5 mmol $NaBH_4$, 5 mL THF; *b*- 50 mg of **3**, 1 mmol KOH, 4 mmol KF, 3 mmol CaC_2, 110 μL H_2O, 3 mL DMSO, 130 °C, 4 h.

Scheme S2. Vinylation of progesterone steroid.

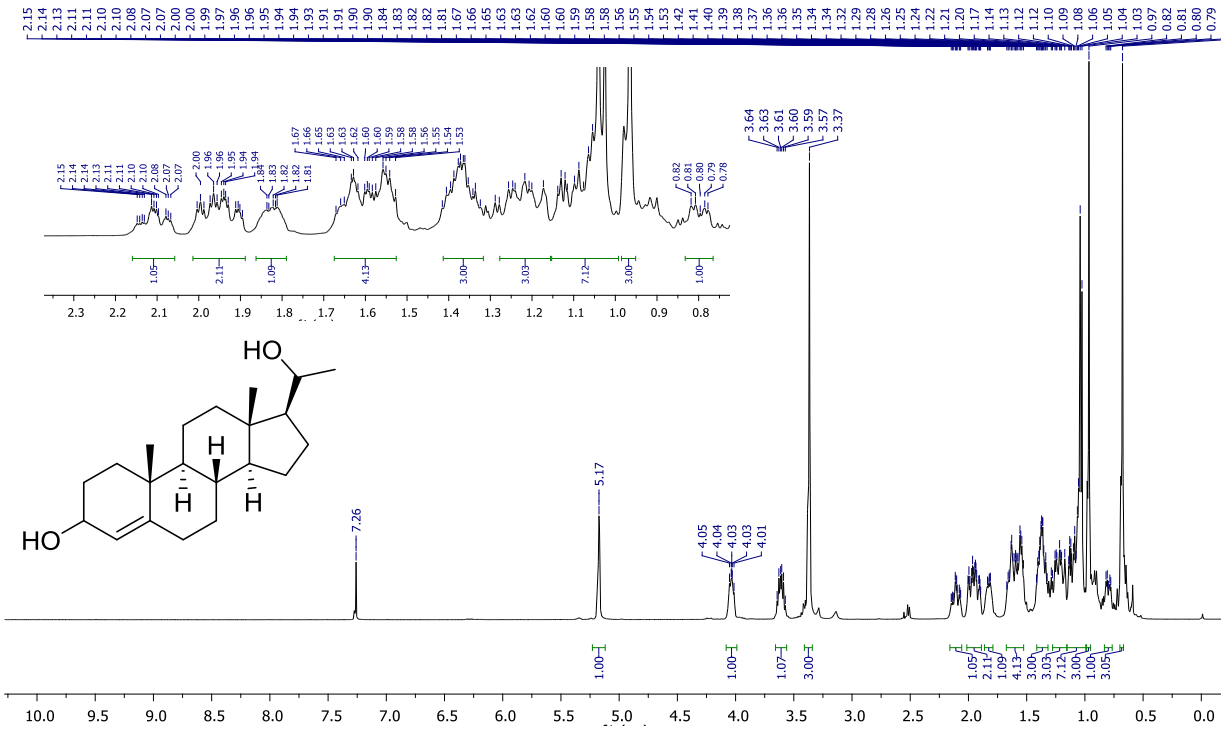

Figure S37. ^1H NMR spectrum (400 MHz, $CDCl_3$, δ, ppm) of 4-pregnan-3,20-diol (**3**) in $CDCl_3$ (reaction mixture).

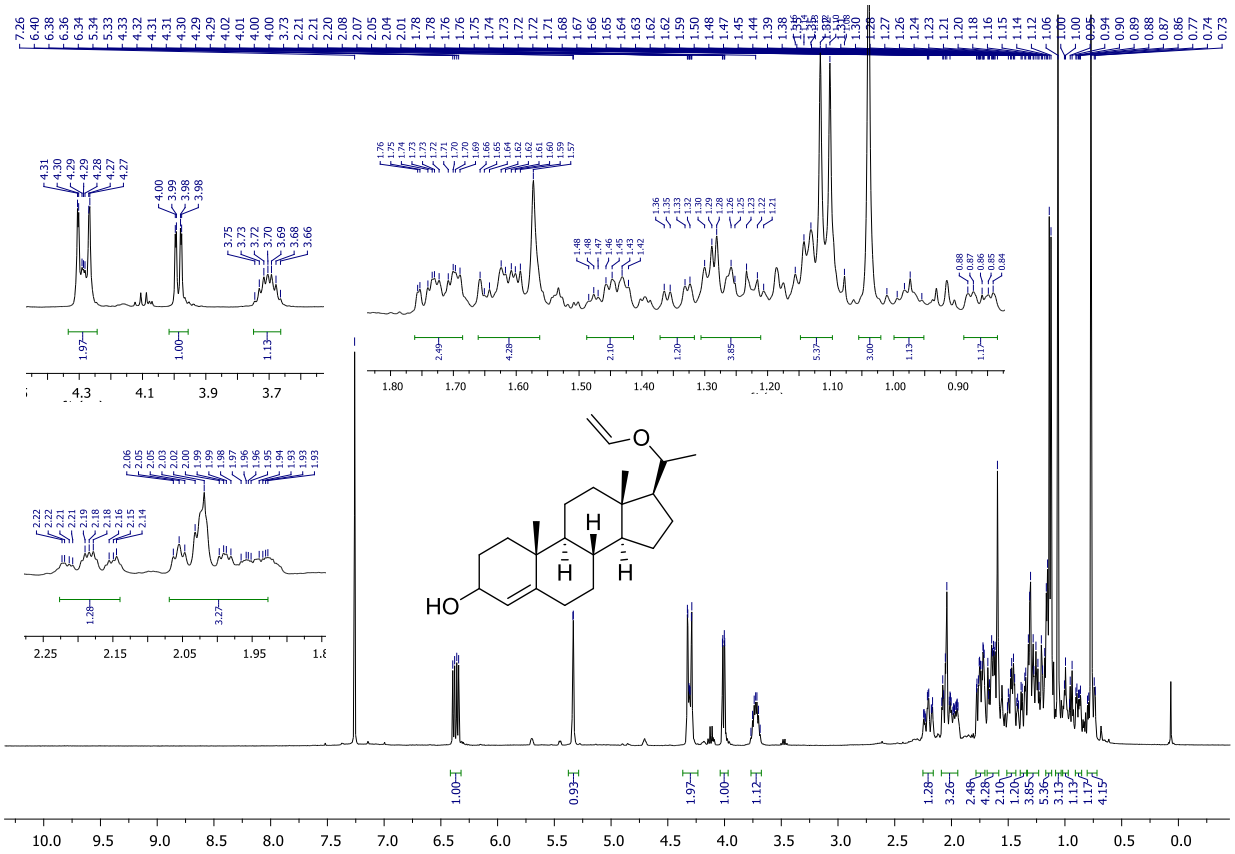

Figure S38. ^{1}H NMR spectrum (400 MHz, $CDCl_3$, δ, ppm) of 20-vinyloxy-4-pregnan-3-ol (**4**) in $CDCl_3$.

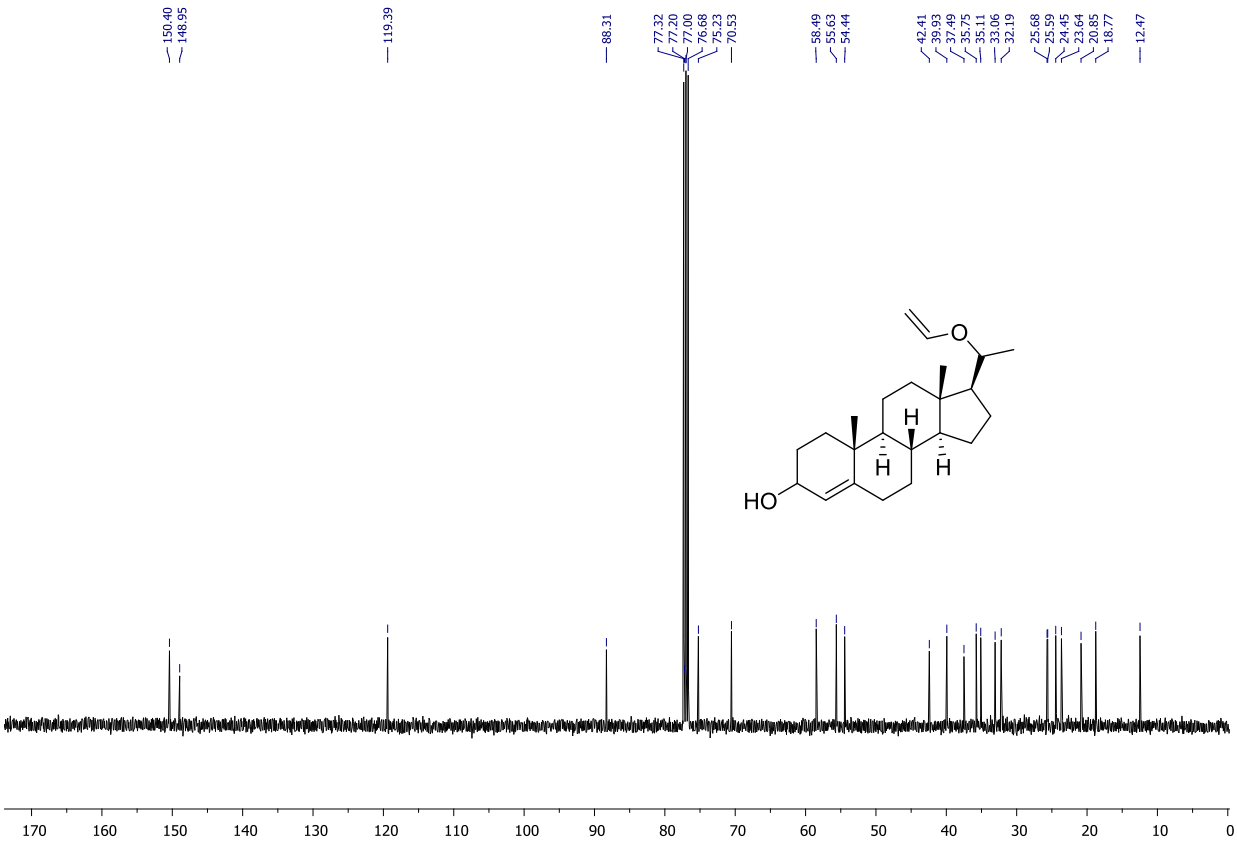

Figure S39. ^{13}C NMR spectrum (101 MHz, $CDCl_3$, δ, ppm) of 20-vinyloxy-4-pregnan-3-ol (**4**) in $CDCl_3$.

5. References

[1] V. A. Korabelnikova, E. G. Gordeev, V. P. Ananikov, Systematic study of FFF materials for digitalizing chemical reactors with 3D printing: superior performance of carbon-filled polyamide, *React. Chem. Eng.*, 2023, **8**, 1613-1628, DOI: 10.1039/D2RE00395C.
[2] W. Zhang, J. Du, G. Xu, H. Lin, G. Wang and M. Tao, *Green Chem*., 2016, **18**, 2726-2735, DOI: 10.1039/C5GC02621K.